THE ELECTRODEPOSITION OF SILVER AND IRON.

By

D.N.LAYTON.

Thesis Submitted for the Degree of
Master of Science in the University
of London.

Applied Physical Chemistry Laboratories,
Imperial College, London, S.W.7.

July, 1950.

Contents

LIST OF FIGURES

41. F 3950

42. V 257

43. F 4396

44. F 4397

45. F 4377

46. F 4378

47. Diagram, indexing of figure 45

48. Diagram, [11$\bar{2}$] rotation twin

49. Diagram, twins about 310 axes in plane of diagram

50. Diagram, twins about 310 axes not in plane of diagram

51. V 311

52. V 367

53. F 4320

54. F 4322

55. V 307

56. V 306

57. V 363

58. F 4725

59. V 361

60. F 4769

61. F 3578

62. J 2068

63. F 3589

64. Diagram, (113) orientation

65. Diagram, (112) orientation

66. V 274

67. 286/4

68. V 284

69. V 273

70. F 4104

71. F 4099

72. F 4098

73. F 4452

74. F 4475

75. F 4493

76. F 4494

77. F 4514

78. F 4629

79. F 4601

80. F 4606

Abstract of Thesis

The Electrodeposition of Iron and Silver.

By D.N.Layton.

It is now known that electrodeposits grow under two main and conflicting influences connected with the substrate and bath conditions respectively. The form of growth promoted directly by the bath conditions (cationic concentration etc.) is invariably one exhibiting, at most, only one degree of orientation. This orientation may be such that the crystals either grow laterally, with the most densely packed atomic plane parallel to the plane substrate, or outwards in such a manner that the common axis of orientation is normal to the surface and consists of an atom row of high (generally maximal) atom frequency. If the substrate is crystalline and the bath conditions favour lateral growth, the first layers of the deposit, up to a few hundred angstroms in thickness, may grow so as to continue, more or less faithfully, the structure of the substrate. Under favourable conditions the structure may be continued throughout a deposit thickness of 100,000 A., and possibly much more. On the other hand, if the bath conditions favour outward growth, the deposit grows, even on an active substrate, as crystals having only one degree of orientation.

In the present work the effects of current density and ion concentration on the growth of silver deposits from a silver nitrate bath were studied. It is shown that at high current densities the silver grows away from cation-depleted regions as needle-like crystals penetrating into regions of high Ag^+ ion concentration. At low current densities lateral growth predominates.

The effects of bath conditions on the growth of electrodeposits of iron on single-crystal and polycrystalline iron were also studied. Under conditions which favour the production of a one degree orientation with the most densely packed atomic plane parallel to the substrate (lateral growth) the deposit continued the structure of an iron single-crystal substrate fairly well to thicknesses of 55,000 A. at least. Modifications of this type of growth, and various other one degree orientations produced by different bath conditions were observed and their significance is discussed.

Introduction.

Since the discovery of X-ray and electron diffraction several workers have investigated the variations in crystal orientation and structure of electrodeposited metals produced under different conditions [1-11]. Optical microscopy, which had previously been much used, yields evidence which, on its own, is generally incomplete and inconclusive, and may even be directly misleading [7]. X-ray and electron diffraction and more particularly the latter, can, however, give complete evidence of the nature of crystalline structure and orientation. Electron diffraction is much superior to X ray diffraction because, owing to the low penetration of electrons, changes in structure and orientation can be followed step-by-step as the deposit thickness is increased.

In particular, Finch and his collaborators [6-9] who have carried out the first and, up to the present, the only systematic study of the growth and structure of electrodeposits have obtained results which afford a clear picture of cathodic crystalline growth. They have established that the two main influences governing the structure of an electrodeposit are those of the substrate and those of the bath conditions and that these act in opposition to each other. The substrate influence, if dominating, causes the deposit crystals to grow

epitaxially* and may also control the crystal size. If the bath conditions take charge the crystal orientation and size are unrelated to those of the substrate and wholly determined by the bath conditions.

It has been suggested [12] that metal ions may be discharged where they approach the cathode and then migrate to a position of minimum potential energy, unless prevented from doing so by low temperature or adsorbed material. The impossibility of this mechanism is obvious since the mobility of atoms on the surface of a solid at the temperatures used in electrodeposition is very small. Nor would it be possible for atoms deposited in unstable positions to re-enter the solution as ions and be deposited elsewhere since the rate of dissolution of a metal which is more negative than its reversible potential with respect to the solution in which it is immersed is infinitesimal. The ions must therefore be transported in the solution next to the cathode by thermal motion of the solution until dehydration and discharge can occur at a stable position. These stable positions of minimum potential energy will be at the edges of the most densely packed atom planes. The work necessary to achieve the final state will appear as an overvoltage in the metal deposition.

---

* Epitaxy - "orderly arrangement on". The orientation of the deposit crystals is such as to achieve good atomic fitting across the deposit-substrate interface.

If the substrate is crystalline, the initial layers of the deposit will also be crystalline if the deposition conditions permit, normally having their own characteristic structure, though cases of pseudomorphism [10] have been reported. The deposit crystals will be disposed on the substrate so as to achieve the best possible atomic fitting at the interface, differences of atomic spacing in parallel directions up to 15%, and possibly much more, being tolerated. Such epitaxial growth has been observed in deposits of silver, gold, cobalt, nickel and copper on single crystals of copper, gold, silver and iron on iron single crystals [8], bismuth, antimony and silver on bismuth single crystals, tin on tin single crystals, and antimony on antimony single crystals [9]. Good atomic fitting was achieved in deposits of gold and silver on a (110) face, and of silver on a (001) face, of iron single crystals by the (001) planes of gold or silver forming parallel to the (110) planes of iron with the [010] atom rows of gold or silver parallel to the [001] rows of iron [8]. Similarly, cases of parallel growth, or orientation to produce good atomic fitting, have been found in deposits on orientated polycrystalline substrates [6].

A polished metal substrate presents a smooth amorphous surface, so the initial layers of the deposit will also be

amorphous. However, the irregular groupings of atoms in these amorphous layers will act as crystal nuclei, and the deposit will subsequently become crystalline if the bath conditions allow.

There are many factors in the bath and deposition conditions which may affect the growth of electrodeposits such as temperature, nature, concentration and rates of diffusion of both the cation and anion, current density and efficiency, ion-association, overvoltages at the electrodes, stirring, and the presence of other materials (e.g. colloids or basic hydroxides) which may also be deposited on the cathode. Some of these variables are interdependent: thus variations of temperature affect the rate of ionic diffusion, current efficiency, and overvoltage, and variations of current density may also affect the current efficiency and overvoltage. The nature of the cation usually has a profound effect on the deposit, e.g. good deposits of iron may be obtained from baths containing the ferrous ion but not from those containing the ferric ion. The combined effect of all these factors is to promote a particular type of structure in the deposited metal which may be amorphous or crystalline (either random or orientated).

Amorphous deposits are not common, but they have been

observed in the case of metals with weak cohesive forces (e.g. antimony, arsenic and selenium) when the process of lattice formation has been seriously disturbed by an accumulation of hydrogen ions or atoms on the cathode because of a high hydrogen overvoltage, or by an excessive evolution of hydrogen [8]. Metals with greater cohesive forces (as shown by higher melting-point and surface tension) formed random crystalline deposits under such conditions. It has further been shown that random deposits of metals, with high hydrogen overvoltages, such as zinc, cadmium and lead, were always obtained under conditions of accumulated hydrogen ions or atoms, but in some cases increasing the current density, and thereby making the cathode more negative, caused the hydrogen to be evolved and the deposit became orientated.

When orientation occurs in a thick polycrystalline metal electrodeposit it is invariably only one-degree. Two main types of such crystal growth have been distinguished - lateral growth, in which the crystals grow with the most densely packed atomic plane parallel to the substrate, and outward growth in which the crystals grow so that their common axis of orientation is normal to the substrate and consists of an atom row of high (generally maximal) atom frequency.

Lateral growth occurs when the rate of deposition of ions on the cathode is not too high compared with the rate of supply of ions to the cathode region by diffusion and migration, i.e. the ionic concentration in the solution adjacent to the cathode is high, and the ions are not prevented from migrating over the cathode surface and being freely discharged by adsorbed materials. It is therefore favoured by high ion concentration, high bath temperature, low current density, and stirring, or a combination of these conditions. Those crystals having the most densely packed planes parallel to the substrate then tend to grow sideways more rapidly than those with other orientations and receive a greater proportion of the incident ions. If, on the other hand, the rate of supply of ions to the cathode region is not very high, or the mobility of the ions over the cathode surface is reduced by low temperature or adsorbed material, some form of outward growth will probably occur.

Under bath conditions which favour lateral growth, an electrodeposited metal may continue the structure of a single crystal cathode to considerable deposit thicknesses ($\sim$100,000 A. [9] but under less favourable circumstances the deposit may become polycrystalline with an orientation characteristic of the deposition conditions after a thickness of only a few hundred angstroms.

Some attempts have been made to correlate bath conditions with the structure, stress and mechanical properties of electrodeposits, but where these have been studied simultaneously, the structure has usually been inferred only from microscopical evidence, and much doubt remains as to the exact orientation of the crystals.

It is therefore clear that although our knowledge of the mechanism of electrodeposition has increased considerably in recent years, the problem is a very complex one and much still remains to be learned. The present work aims to elucidate some of the effects of the conditions prevailing in the electrolytic bath on the growth of electrodeposits. Accordingly, the effects of variations in ionic concentration, bath temperature and current density on the growth of silver and iron deposits were studied. Optical microscopy, electron diffraction and, to a limited extent, electron microscopy, were used to observe the structure and habit of the deposits in order to obtain the fullest information possible. The diffraction camera was of the Finch type and has been fully described elsewhere together with an explanation of the interpretation of electron diffraction patterns [13].

The experimental work is conveniently divided into two parts, on silver and iron respectively, and the general

conclusions discussed later. During the course of the work on iron it was considered desirable to investigate the deformation of iron crystals by the recently defined process of rotational slip and the results of this research constitute Part III of the thesis.

PART ONE.

THE ELECTRODEPOSITION OF SILVER.

Part I. The Electrodeposition of Silver.

Historical.

Most early work on the deposition of silver was concerned with the production of commercial electroplate or electro-refining processes, and has been fully reviewed by Frary [14]. Electrodeposits from silver nitrate baths are coarsely crystalline and hence unsuitable for commercial work, but the ease with which the crystals could be observed with the microscope has resulted in a number of people using this simple bath to study crystal growth by electrodeposition.

Le Blanc [15] in 1910 used an oscillographic method to investigate anodic and cathodic voltages for a number of metals immersed in solutions of their salts during the passage of current. With an alternating current of 56 cycles per second he found for silver that the rise in voltage was the same at both the anode and the cathode, but was greater in a normal solution of silver nitrate than in one which was also normal with respect to nitric acid. Aten and Beorlage [16] observed that in the electrolytic growth of silver deposits from the nitrate solution the number of nuclei was increased by any alteration in the bath conditions which increased the concentration polarisation, e.g. decreasing the ionic

concentration, increasing the current density, or acidifying the solution. They also found that the number of nuclei was increased by the addition of gelatin to the solution, a fact later confirmed by Wernick [17] who studied the effects of a number of other additions to the silver nitrate bath.

Hoekstra [18] considered that the interpretation of the logarithmic relation between overvoltage and current density in terms of concentration polarisation was unsound and found that with continuous scraping of the cathode the overvoltage was directly proportional to the current density and concluded that the other forms of overvoltage-current density relationships were the result of the adsorption of impurities on the cathode. He ignored, however, the stirring of the solution which inevitably resulted from the scraping process, and if the effects of concentration polarisation are eliminated a linear relationship, as a result of a slow process in deposition, is not surprising. Hoekstra also observed the growth of silver crystals in layers about a thousand atoms thick, the number of layers and their rate of movement across the surface during growth increasing with increasing polarisation, and the fact that this type of growth was modified if the deposition was stopped for some time. This last effect was explained as passivation by adsorption of

impurities on the growing edges.

The passivation of silver cathodes during interrupted growth has been studied by several other workers, and the evidence ofVahramian [19] seems conclusive in support of the explanation that it results from the adsorption of impurities.

The discrepancies between the overvoltage relationships with current density reported by different observers was attributed by Vahramian [19] to the "apparent" rather than the "true" current density having been considered. His own measurement of the "true" area of deposition of a single growing filament by dividing the volume of silver deposited by the increase in length of the filament is open to objection since it neglects the deposition which occurs on the sides of the filament. The present work indicates, however, that if the growth is at all rapid, the rate of deposition on the sides of the filament is in fact small compared with the rate of deposition on the tip, and Vahramian's results may therefore not be completely invalid. He found that the overvoltage was a linear function of the logarithm of the "true" current density and concluded that it was due to concentration polarisation.

Growth of silver crystals in layers has also been observed by Vahramian, and evidence suggesting the existence of

concentration gradients on the face of a growing crystal, as would be expected with this type of growth, has been reported by Gorbunova [20]. In the face of these direct experimental observations the theoretical model devised by Fischer [21] to explain the production of "layered" crystals as a result of growth proceeding alternately on horizontal and vertical faces seems of little value, as well as being improbable.

Glocker and Kaupp [2] found by X-ray diffraction that silver deposited from a cyanide bath at 7 mA./sq.cm., or from a N/10 silver nitrate solution at 22 mA./sq.cm., was random, but when deposited from N/10 silver nitrate at 10 mA./sq.cm. the silver was coarsely crystalline, and some of the crystals were in (111) or (001) orientation. They suggested that growth with a preferred orientation only occurred when the ratio of the number of nuclei relative to the rate of deposition was within a certain range which was smaller the more nearly equal were the velocities of growth in different crystallographic directions.

Finch and Sun [6] found that silver deposited from a cyanide bath at a current density of 10 mA./sq.cm. on to polycrystalline gold in (111) orientation was also in (111) orientation, and Finch, Wilman and Yang [8] using a similar bath and a polished brass cathode obtained silver in (111)

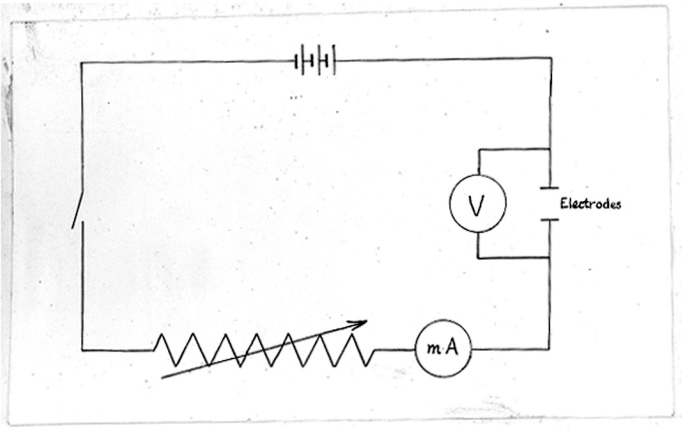

Figure 1. Circuit diagram.

orientation (i.e. lateral growth) at a current density of 1 mA./sq.cm. and in (110) orientation (outward growth) at a current density of 30 mA./sq.cm.

In order to discover in more detail how the concentration of the electrolyte and current density affected the formation of electrodeposits, the growth of silver from silver nitrate solutions on various types of cathode was observed by means of a microscope, and the observations correlated as far as possible with the results of electron diffraction examinations.

Experimental.

The electrodeposition was carried out partly in a 150 cc. beaker in the side of which a hole had been made and covered with a glass cover slip, and partly in a rectangular perspex tank of about the same capacity. The electrical circuit is shown in Figure 1. The milliammeter was calibrated on both the 5 mA. and 50 mA. ranges with a copper coulommeter.

The cathodes used in most of the work were (i) the edge of a copper sheet 1 mm. thick, the rest of the sheet being covered with polythene, (ii) a horizontal copper wire (14 S.W.G.) (iii) the edge of a silver sheet (16 S.W.G.), and (iv) the flat or pointed tip of a silver wire (20 S.W.G.). In cases (ii),

(iii) and (iv) parts on which a deposit was not wanted were blocked off with collodion. Silver cathodes were chiefly used to avoid the possibility of silver being deposited by displacement which might affect the growth of the initial crystals and would result in the contamination of the electrolyte with copper. In every case the growth of the deposit was observed through a travelling microscope and photomicrographs of the crystals were taken, using Kodak 0.250 plates. The electrolytic cell and microscope were insulated from vibration by placing them on a stout wooden board mounted on 1/4" blocks of medium-hard rubber and pads of filter paper.

For examination by electron diffraction some deposits were produced on silver sheet polished with "Bluebell" and on an approximate cube face of an electropolished iron single crystal. The preparation of iron single crystal surfaces for electrodeposition is described in Part II.

Results and Conclusions.

The observations of electrodeposits from N/2 silver nitrate solution are summarised in Tables I and II. The current densities shown in Table I are the apparent ones obtained by dividing the current by the area of the cathode and are included merely for comparison. As the deposit grew

Table I.

Electro-deposition from N/2 $AgNO_3$ solution at constant current.

Apparent c.d. mA/sq.cm	P.d. between electrodes. volts.	Type of growth of deposit	Fig.	Cathod
1 - 45	0.05	Slow growth of small squat crystals. Some appeared to be octahedra lying on a triangular face.	5,6, 7,8.	(i) (ii) (iii)
120-250	0.08	Initially rapid growth of small needles, but these started thickening after about 2 or 3 sec. and stopped rapid longitudinal growth.	10	(i) (iii) (iv)
500-750	0.4 falling to 0.12	Initially needles, but these tended to become blunt and thick, though some continued rapid growth.	11,12 13,14	(iii) (iv)
800-1500	0.5 falling to 0.3	Prolific needle growth at first giving way to a more even development of crystals although some needles continued as such.	15	(iii) (iv)
2000	0.7 falling to 0.4	Prolific needle growth, many of them branched.	16,17	(iii)

Table II.

Electrodeposition from N/2 $AgNO_3$ solution at constant voltage.

Voltage	Type of deposit	Fig.	Cathode.
0.2	3 or 4 crystals grew as needles Most of cathode covered with small crystals.	18	(iv)
0.3	Large number of crystals grew as needles.	19,20, 21,22	(iii) (iv)
0.6	Rapid fern-like growth of crystals. Deposit very loose.	23	(iv)
0.8	Do.	24	(iv)

the true current density decreased causing the overvoltage of concentration polarisation also to decrease, as is indicated by the fall in voltage recorded in the second column of Table I. This decrease in current density was responsible for the changes observed in the growth of deposits at constant current since the initial type of growth was maintained when the voltage was kept constant by increasing the total current.

The two main features observed in the deposition of silver were the slow steady growth of all the crystals at low current densities and the rapid extension to needle-like form of some crystals at high current densities; the number of crystals growing in such a manner increasing with increasing current density. At very high current densities the deposit consisted of many small crystals and had the general appearance of a fern growth.

After the examination of many individual crystals it was concluded that the length of the needle-like crystals was parallel to a [110] direction (i.e. parallel to the densest atom rows), and that when "branching" occurred it was along other equivalent [110] directions at 60° to each other. The length of some silver "wires" is also reported to be parallel to [110] [22]. The sides of the needles were {111} faces, at least in part, (if not {111} they would have to be of {11ℓ}

type). It was not possible to determine a precise orientation of the remaining small crystals or of the crystals formed at low current densities, though some of the latter appeared to be octahedra growing with a {111} face parallel to the cathode.

It was impossible to obtain electron diffraction patterns from deposits grown on polished silver sheets from nitrate baths at current densities of 1 mA./sq.cm. or 0.1 mA./sq.cm. because the deposit was in the form of isolated crystals growing at imperfections, such as scratches or pits, in the polish layer. Such imperfections would exhibit the crystalline structure of the silver sheet and preferential growth would occur there since atoms completely ordered as crystals have less potential energy. This effect has been demonstrated by the work of Coffin and Tingley [23] on ion-exchange between silver sheets and nitrate solutions in which they were immersed. In any case deposits formed on the polished part would be at first amorphous or microcrystalline and not yield a diffraction pattern. Similar growth at isolated points on polished surfaces has been observed by Gorbunova and Vahramian [24].

It was realised from previous work that bath conditions favouring lateral growth were likely to result in an epitaxial deposit on a crystalline cathode, and silver was therefore

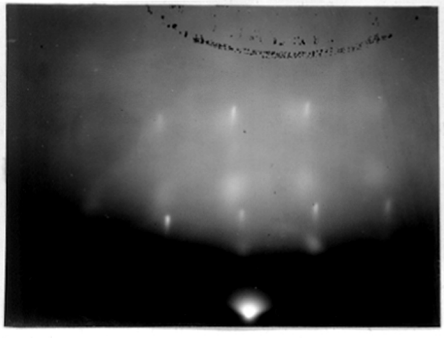

Figure 2. Ag deposited on Fe approx. (001) face from N/2 $AgNO_3$ at 0.5 mA/cm^2.

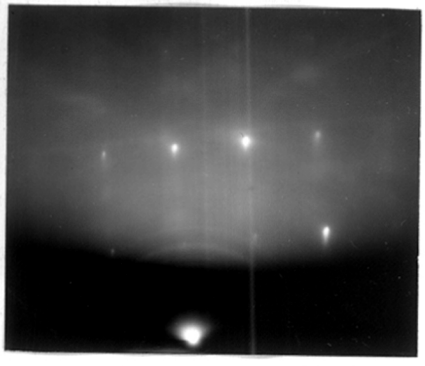

Figure 3. Ag deposited on Fe approx. (001) face from N/2 $AgNO_3$ at 1 mA/cm^2.

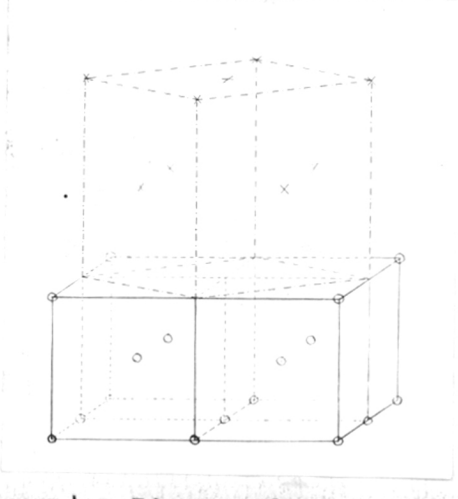

Figure 4. Diagram showing epitaxial arrangement of Ag lattice on Fe.

deposited from N/2 silver nitrate solution on an electropolished approximate cube face of an iron single crystal at current densities of 0.5 mA./sq.cm. and 1 mA./sq.cm. The electron diffraction patterns from these deposits are shown in Figures 2 and 3. In Figure 2 the $\sqrt{2}$-rectangle pattern of spots elongated perpendicular to the shadow edge is due to the iron, and the square pattern of rather diffuse spots is due to silver, showing clearly that the cube face of silver had grown parallel to that of iron but rotated through 45° so that the cube edge of silver was parallel to the cube face diagonal of iron (see Figure 4). Examination with a metallurgical microscope showed that the silver deposit was in the form of discrete crystals, and their orientation was the same as that deduced from the electron diffraction patterns. The thickness of the individual crystals was too great to allow a photomicrograph to be taken. Figure 3 shows that the crystals of silver formed at 1 mA./sq.cm. were randomly disposed and this conclusion was also confirmed by microscopical examination.

It therefore seems that at nominal current densities of 0.5 mA./sq,cm., or less, lateral growth occurs from the N/2 silver nitrate bath. In fact, the true current density must have been greater than this value because the number of actual growing nuclei was small (cf. Figure 8 for example). At

Figure 5. 5 min. deposit from N/2 $AgNO_3$ at 45 mA/cm^2. X50

Figure 6. Further 25 min. deposit on that of figure 5. X50

Figure 7. Further 45 min. deposit on that of figure 6. X26

Figure 8. 13 hour deposit from N/2 $AgNO_3$ at 0.1 mA/cm^2. X75

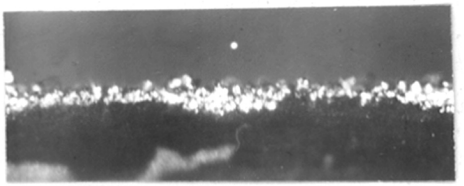

Figure 9. 7 min. deposit from N/10 $AgNO_3$ at 50 mA/cm^2. X75

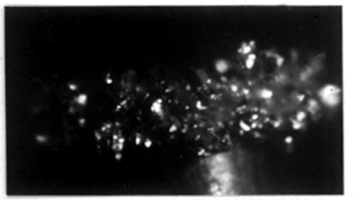

Figure 10. 30 min. deposit from N/2 $AgNO_3$ at 130 mA/cm^2. X39

Figure 11. 20 sec. deposit from N/2 $AgNO_3$ at 750 mA/cm^2.
X39

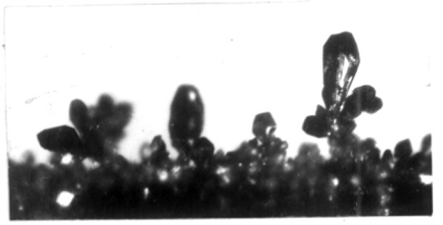

Figure 12. Further 5 min. deposit on that of figure 11.
X39

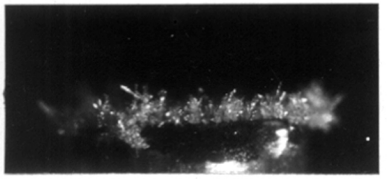

Figure 13. 15 sec. deposit from N/2 $AgNO_3$ at 480 mA/cm^2.
X39

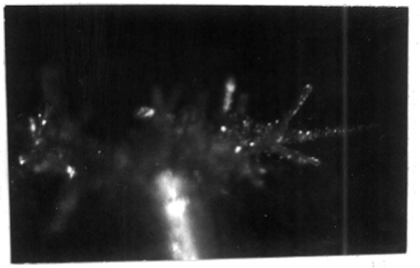

Figure 14. As figure 13, but 1 min. deposit.
X39

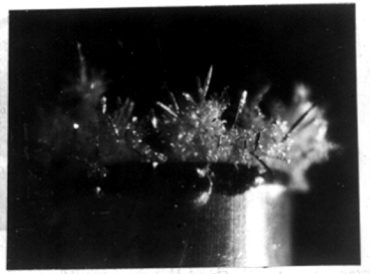

Figure 15. 15 sec. deposit from N/2 $AgNO_3$ at 800 mA/cm^2.
X39

slightly higher current densities the growth was random. It will be seen from Figures 5, 6 and 7 that although the deposit is coarsely crystalline, the crystals have grown fairly rapidly and without any obviously preferred orientation. The deposit from N/10 silver nitrate solution at the same current densities was similar, but a comparison of Figures 5 and 9 shows that the number of nuclei was much greater in the more dilute solution. The deposit at current densities a little higher still were initially as shown in Figure 11, but as the actual current density fell the crystals developed more uniformly (Figure 12) though nevertheless maintaining a form of outward growth.

More obvious outward growth in the form of needles occurred at much higher current densities (Figures 15, 16 and 17), and the fact that the needles did not always grow normal to the cathode suggests that ionic concentration is the chief factor controlling the direction of growth. If during the deposition at these high current densities the current was reduced to about one-fifth, the needle-like crystals became thicker and blunt at the tip. Subsequent restoration of the current to its former value did not result in a resumption of needle growth but only in a more rapid general development of all the crystals. If, however, the current was switched off, needle growth continued unaffected when it was switched on

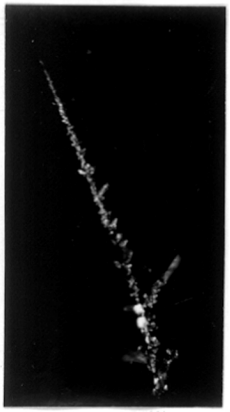

Figure 16. 1 min. deposit from N/2 $AgNO_3$ at 2000 mA./cm^2. x 25

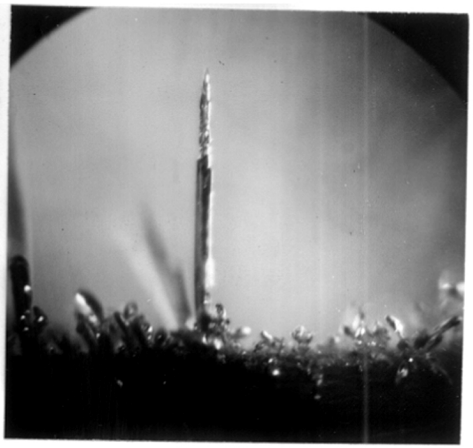

Figure 17. As Figure 16, but 20 sec. deposit x 39

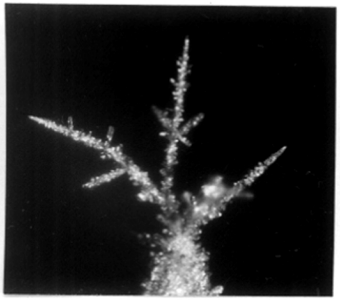

Figure 18. 1 min. deposit from N/2 $AgNO_3$ at constant voltage (v=0.2 volt) x39

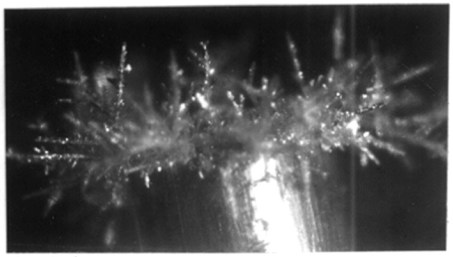

Figure 19. 1 min. deposit from N/2 $AgNO_3$ at constant voltage (v= 0.3 volt) x 39.

again a few minuted later. Needle-growth did not continue if the current was left off for a period of about half an hour.

The usual explanations of "treeing" in electrodeposits are that the ohmic resistance of the solution between projections and the anode is less than of that between the rest of the cathode and the anode, and therefore a large proportion of the current is carried by the projections, or that the electrostatic field is more intense at the projections and therefore the rate of deposition is increased. The effect of differential resistance is probably one of the causes of uneven deposits in some cases, but the conductivity of most electrolytes is sufficiently high that the effect will not be great, and it may in any case be offset by a higher voltage being required to maintain the increased current density at the projection (e.g. because of concentration polarisation) so that if the potential difference applied to the cell is constant, the deposit will tend to grow more uniformly over the whole cathode. It is in fact generally agreed that an electrolytic bath in which the cathode potential rises rapidly with current density is likely to have a good "throwing power" [25, 26].

The modifications to charge distribution and field strength caused by projections on a conductor are well known

on a macroscopic scale, but it is difficult to predict the effects of projections of the order of atomic dimensions. However, intense fields may be set up at such excresences, but they will undoubtedly be very local compared with the thickness of the diffusion layer (of the order of $\frac{1}{2}$ mm.). Most ions have a mobility of about 5×10^{-4} cm./sec. under a potential gradient of 1 volt/cm. at infinite dilution, and potential gradients of the order of 100,000 volts/cm. are required before the retarding effect of the oppositely charged ionic atmosphere is overcome. Hence the only possible effect of the intensification of the electric field at minute projections would be a more rapid removal of ions from the diffusion layer in the immediate neighbourhood than would occur at an atomically smooth cathode. The supply of ions to the diffusion layer will, however, be unaffected. That the effect of variations in the electric field is very local was shown by arranging a growing needle on the pointed silver wire cathode with its tip about 1.5 mm. from the anode. The experiment was tried several times, and on each occasion the needle continued its growth quite independently of the position of the anode although sometimes approaching very close to it, and some branches even grew in the opposite direction.

At the instant of switching the current on, a rapid

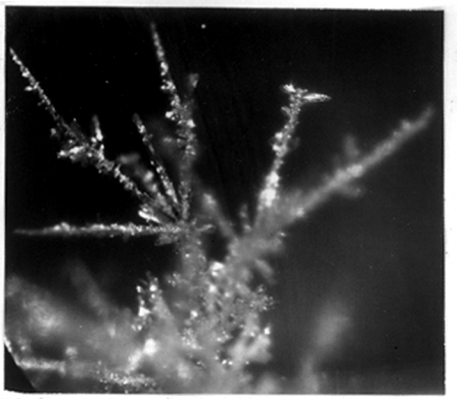

Figure 20. Further 1½ min. deposit on that of Figure 19. x39

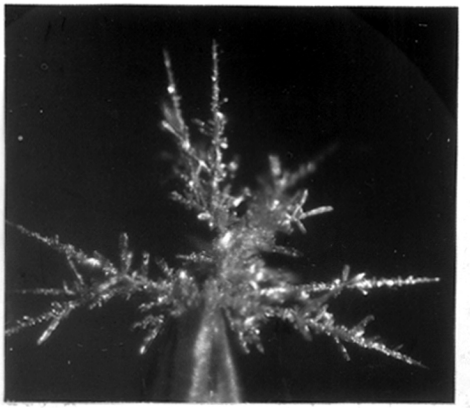

Figure 21. 1 min. deposit from N/2 $AgNO_3$ at constant voltage (v= 0.3 volt) on pointed wire. x 39.

deposition of the ions immediately next to the cathode occurred, leaving the solution in that region impoverished. Some of the crystals having the densest atom row perpendicular, or nearly so, to the cathode grew enough to have their tips sufficiently far from the immediate neighbourhood of the other crystals to be in regions where the cation concentration was still high and approximately equal to that in the bulk of the solution. Rapid growth of such crystals was then maintained since only a relatively small number of ions was required for the longitudinal extension of the pointed needles, and the concentration polarisation at the tips was therefore much smaller than at all other crystal surfaces in the deposit. Because of the large reduction in ionic concentration elsewhere, the rest of the deposit only grew slowly.

A substantial reduction in the current density, either by reduction in the current flowing in the external circuit or by the increase in surface area as the deposit developed, resulted in the slow growth of the tips which developed larger distinct crystal faces, and all the crystals in the deposit then grew more evenly (Figure 12). Once the ends of the needles had become blunted in this way, subsequent restoration of the current to its former value did not result in a resumption of the needle growth since the number of ions required for the longitudinal extension of the crystals was

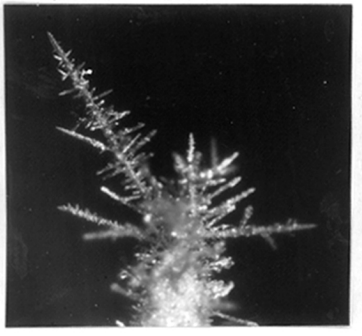

Figure 22. As Figure 21 but 30 sec. deposit x39.

Figure 23. 30 sec. deposit from N/2 $AgNO_3$ at constant voltage (v= 0.6 volt) x39.

Figure 24. 1 min. deposit from N/2 $AgNO_3$ at constant voltage (v= 0.8 volt) x39

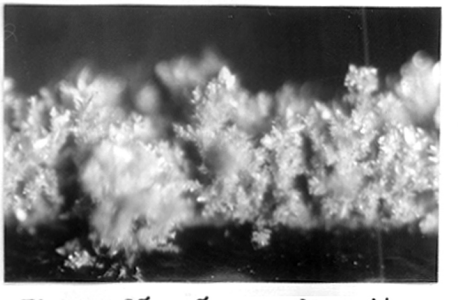

Figure 25. 5 sec. deposit from N/10 $AgNO_3$ at 2000 mA./sq.cm. x 60.

then relatively great and the cation concentration was rapidly reduced at the ends of the crystals as well as at the other surfaces. If the current was completely stopped for a short time, however, the shape of the crystals remained unaltered and needle growth continued unimpaired when the current was switched on again.

Since no special precautions were taken to ensure the purity of the bath, the failure of needle growth to continue after a complete stoppage of deposition for a long period was probably due to the adsorption of surface active materials on the growing surfaces at the tips.

By gradually increasing the current in the external circuit as the deposit grew, to keep the potential difference between the electrodes constant, the current density and concentration polarisation were maintained at steady values and the initial type of crystal growth continued unaffected throughout the deposition.

At very high current densities the deposit consisted of a loose fern-like aggregation of many small crystals (Figures 23 and 24). This was the result of the rapid growth of such a large number of nuclei that the immediately surrounding solution was completely starved of silver ions and

continued growth of the crystals was impossible.

The conclusion that cationic concentration is the chief controlling factor in the growth of the deposits was confirmed by experiments with N/10 silver nitrate solution from which it was impossible to maintain needle growth. Though such growth occurred initially it subsequently became fern-like (Figure 25) at a current about one-fortieth of that necessary to produce fern growth from N/2 solution, because of the more rapid reduction of ionic concentration at the growing surfaces in this dilute solution. Not only is the total ionic concentration less, but the fraction of ions associated as ion-pairs in N/10 silver nitrate is only 0.048 compared with 0.14 in the N/2 solution [26], so that partial restoration of the silver ion concentration by further dissociation cannot take place to any appreciable extent in the former solution.

PART TWO.

THE ELECTRODEPOSITION OF IRON.

Part II. The Electrodeposition of Iron.

Historical.

The first systematic work on the electrodeposition of iron was that of Alexander Watts [27] who published in 1880 the results of his investigation of the use of baths containing one or more of 44 different compounds of iron, and concluded that satisfactory deposits could only be obtained from baths containing the ferrous ion. Subsequent developments in iron electrodeposition were exhaustively reviewed by Hughes in 1921 [28].

Burgess and O.P.Watts [29] studied the microstructure of electrolytic iron and noted that it consisted of crystals generally elongated in a direction perpendicular to the cathode and sometimes of nodules and trees. They also found that the appearance of the grains was altered when the deposit was heated to 910°C., a transition point. Müller [30] investigated the production of iron on an industrial scale and concluded that dense deposits were favoured by high bath concentration and low current densities. He observed that long tree-like deposits were formed at high current densities with a dilute bath. More detailed studies on the effects of heating, quenching, annealing and working of electrodeposited iron

were made by Stead and Carpenter [31], and by Storey [32]. Hughes [33] showed that the presence of considerable quantities of hydrochloric acid in a chloride bath rendered the deposit very finely crystalline, and Ruder [34] suggested that the inclusions in electrolytic iron revealed by microscopic examination might account for the lower permeability and higher hysterisis losses as compared with those for iron from other sources.

The mechanical properties of iron (e.g. hardness, tensile strength, etc.) of iron deposits and their variation with conditions of deposition have been the subject of some recent work by Kaspar [35], Thomas [36], Stoddard [37] and Larson, Moulton and Putnam [38], but the conditions used by each author were so different that it is difficult to draw any general conclusions. Kaspar found that the harder deposit, which he obtained at lower temperatures and higher current densities, were fine grained and contained more oxygen. Kreiger [39], in a brief review of iron deposition, concluded that chloride baths were most satisfactory for thick deposits, and recommended that a bath temperature "high enough to prevent the formation of ferrous hydride" should be used. The existence of ferrous hydride as a distinct compound is open to doubt, and since the entry of hydrogen into the iron lattice to form

an interstitial solution is an endothermic reaction a higher bath temperature would favour this reaction. He mentions that some authors have attributed the hardness of iron deposits to ferrous hydride, while others have regarded the hydrogen as occluded and affecting the mechanical properties by restricting the crystal size.

Several workers have investigated the structure of iron by X-ray and electron diffraction. Glocker and Kaupp [2] examined the structure of a number of electrodeposited metals and concluded from X-ray patterns that the crystals were elongated in a direction nromal to the cathode. They found that from a 10% solution of ferrous ammonium sulphate iron was obtained in strong (111) orientation at a current density of 1 mA./sq.cm. but without any orientation at a current density of 15 mA./sq.cm. From a 50% ferrous chloride bath and a current density of 1 mA./sq.cm. iron was deposited with strong (111) orientation at room temperature and was either random or with weak (100) and (110) orientations at a temperature of 100°C. and a current density of 100 mA./sq.cm. When calcium chloride was added, (112) orientation occurred under the last conditions. Bozorth [3] also obtained iron in strong (111) orientation from a ferrous sulphate bath with ammonium chloride added at 50°C. and 50 mA./sq.cm., and suggested that the stress

existing in electrodeposits of iron and several other metals was caused by the co-deposition of hydrogen which subsequently diffused out. No attempt was made by these authors to correlate the conditions of deposition with the orientation produced or to suggest a mechanism of crystal growth by electrodeposition.

Finch and Sun [6] obtained iron in (111) orientation from a ferrous ammonium sulphate bath at 10 mA./sq.cm. and 20°C., and Yang [9], using the same bath, investigated the orientations of iron deposited on polished brass at various current densities and temperatures on a stationary cathode, on a cathode rotated at 3,000 r.p.m., and in a strong magnetic field. The magnetic field did not affect the crystal orientation though it modified the form of the deposit on a macroscopic scale when it was normal to the cathode. It was shown that in this bath the hydrogen ions were more susceptible to concentration polarisation than the ferrous ones, since under all conditions an increase in current density also increased the efficiency, while at constant current density and temperature, high speed rotation of the cathode caused a marked decrease in current efficiency, and that lateral growth did not occur at room temperature although it was readily obtained at 80°C. Iron deposited under conditions for lateral growth (37.5 mA./sq.cm. and 80°C.) on the cube face of an iron crystal continued the single crystal

structure to a deposit thickness of over 100,000 angstroms.

In the present research, iron was deposited on several different iron crystal faces from sulphate and chloride baths and the effect of variations of deposition conditions from the chloride bath on orientation of polycrystalline deposits on polished mild steel were investigated to obtain more detailed information on the operation of the different factors involved.

Experimental.

The iron single crystals used as substrates were in the form of plates about 3 mm. thick and 5 sq.cm. in area. They were cut with a lubricated jeweller's saw from a bar containing several crystals prepared by the "strain-anneal" method. Great care was taken in the clamping and sawing operations to keep the crystals free from distortion by bending or undue pressure. The crystal faces were smoothed carefully by successive abrasion on grades of emery paper from 0 to 3/0 lubricated with benzene, and then electropolished in the usual perchloric acid- acetic anhydride bath [40] to remove the work-hardened surface layer.

Examination of the crystals by electron diffraction at a camera length of 23 cm. yielded patterns such as Figures 26, 28, 31 and 38. The clearness of the Kikuchi lines show the perfection of the crystal lattice and the few elongated spots

lying on narrow Laue zones indicate that the surfaces were atomically smooth over the area grazed by the beam. Before being used as cathodes the crystals were etched for a few seconds in a 1% solution of picric acid in alcohol to remove the oxide layer.

Blanks of mild steel one inch square and 1 inch x $\frac{1}{8}$ inch were also used as cathodes, and these were smoothed on successive grades of emery paper lubricated with benzene and finally polished with "Bluebell" on 4/0 emery, and "Bluebell" and cotton wool. Before being used as cathodes these blanks were degreased in a jet of grease-free crystallisable benzene.

The composition of the baths used is shown in Table III.

Table III.

Bath 1.	$FeCl_2$	450 gm.	These quantities make up about 1200 cc. of solution.
	$CaCl_2$	500 gm.	
	H_2O	750 gm.	
Bath 3.	As Bath 1, but slightly acidified with HCl.		
Bath 2.	As Bath 1, but diluted to half strength.		
Bath 4.	$FeSO_4(NH_4)_2SO_4.6H_2O$	350 g./l.	
	H_2SO_4	2.5 g./l.	

The first bath is frequently used in commercial practice and was patented by Fischer and Langbein in 1909. Analar chemicals

were used throughout.

The ferrous sulphate bath consisted of about 200 cc. of the solution in a 250 cc. beaker. At room temperature, deposition from the first chloride bath was carried out on the small polished steel cathode in about 90 cc. of solution in a 100 cc. beaker (referred to as bath 1a in the following section) and on the large polished steel cathode in about 200 cc. of solution in a dish about 9.5 cm. in diameter (referred to as bath 1b). When higher temperatures were required the beaker and solution were immersed in a water bath and the temperature maintained at the required value within $\pm$ 1°C. Before electrodeposition, the anode (which consisted of iron electrodeposited on to a sheet of soft iron) and cathode were heated in propyl alcohol to the same temperature as the bath.

After deposition the cathode was washed in a jet of boiled distilled water, dried in acetone and immersed in n-propyl alcohol. It was then transferred, wet with alcohol, to the diffraction camera which was evacuated immediately. Current efficiencies were determined by weighing the cathode before and after deposition, and the thickness of the deposit calculated assuming the specific gravity of the electrolytic iron to have the usual value. After electron diffraction patterns had been obtained, the deposits were examined by means of a metallurgical microscope.

In some cases attempts were made to examine the deposits by electron microscopy. Replicas of the surfaces were made using 1.5% and 4% solutions of formvar in dioxan. These replicas could sometimes be stripped by themselves, but it was usually necessary to back them before stripping with collodion which was subsequently dissolved off in amyl acetate. Some electron micrographs are reproduced, but in general this method of examination was not found satisfactory, chiefly because the surface structure was too coarse to be reproduced by a thin film without strain or tearing in the replica. Figure 32 is an electron micrograph from a formvar replica of an electro-polished (321) face iron single crystal, and shows the surface had a slightly granular texture.

Results and Conclusions.

The experimental results for the deposition of iron on to polished mild steel and iron single crystal substrates are set out in Tables IV and V respectively.

Deposition of iron on iron single crystals. It will be seen that under conditions which give rise to an orientation characteristic of lateral growth in polycrystalline deposits on polished steel, the structure of the single crystal substrate is continued to deposit thicknesses of 50,000 angstroms at least, though modifications such as twinning may occur in

Table IV.

Deposition of iron on to polished mild steel substrates.

Bath	Temp.	Current density mA/sq.cm	Thickness A.	Orientation	Current efficiency
1a	room	.25	8,000-48,000	W(110)	85%
	room	.75-2.5	6,000-42,000	M(111)	
	room	4.0-7.5	28,000-52,000	S(113)	82%at7.5mA/cm
	room	10 - 20	7,000-46,000	(112)+(113)	75%at15 mA/cm
	50°C	5 - 11	8,000-26,000	S(110)	
	70°C	5.4-13	7,000-15,000	S(110)	86% at 8mA/cm
1b	room	1.1	23,000	M(110)	
	room	1.5	9,000-48,000	S(111)	As 1(a)
	room	2.25- 5	14,000-23,000	(112)+(113)	
2	room	0.8-7.0	15,000-58,000	S(111)	As 1(a)
	room	8.0	35,000	(112)+(113)	
3	room	.5 - .95	4,000-11,000	(112)+(113) +VW(111)	70% at .5mA/cm
	room	5	7,000	(112)+(113)	*
4	room	5	18,000	(111)	10%

* Efficiency at 5mA/sq.cm. appeared to be about 95%, but since the specimens were much oxidised, this figure is untrustworthy. A copious evolution was observed during deposition.

Table V

Deposition of iron on to iron single crystal substrates

Bath	Crystal face	Current density mA/cm^2	Temp.	Thickness Å	Type of Deposit	Figures
1(a)	(001)	·25	room	45,000	C, T	39, 40
	(321)	·25	"	50,000	C, arcing of spots	41, 42
	(110)	·25	"	200; 1,000	C, T, (310) facets	43-46, 51
	(110)	·25	"	5,000; 55,000	C, R in centre	53-56
	(110)	·25	70°C.	750	C	52
	(110)	11	70°C.	22,000	C, T	57
	About 10° off (001) face	6·7	70°C.	12,000	C	58, 59
4	(110)	5	80°C.	30,000	C, K	27
	(310)	5	80°C.	30,000	C, K	29, 30
	(321)	5	80°C.	5,000-33,000	C, K	33-36
	(332)	5	80°C.	5,000	C, K	
	(001)	5	20°C.	500	C, R	
	(321)	5	20°C.	500	C, R	37
	{332}	5	20°C.	500	C, R	

C = deposit crystals continued the crystal lattice of the substrate

K = Kikuchi line pattern showing perfect lattice and relatively smooth surface

T = twinning of some of the deposit crystals

R = randomly disposed crystals.

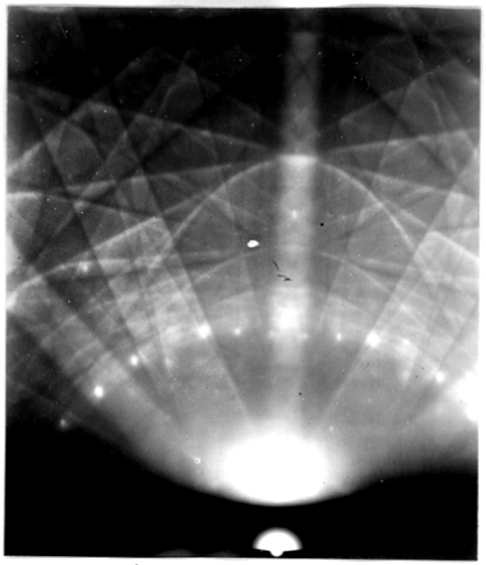

Figure 26. Electropolished Fe (110) face, beam along [001].

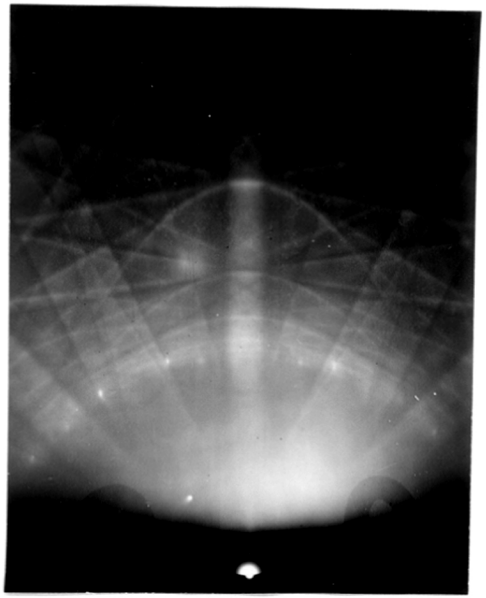

Figure 27. 30,000 A. deposit on Fe (110) face from sulphate bath at 80°C.

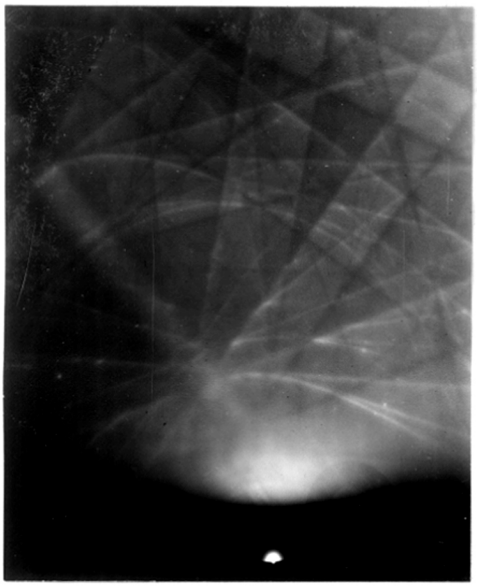

Figure 28. Electropolished Fe (310) face.

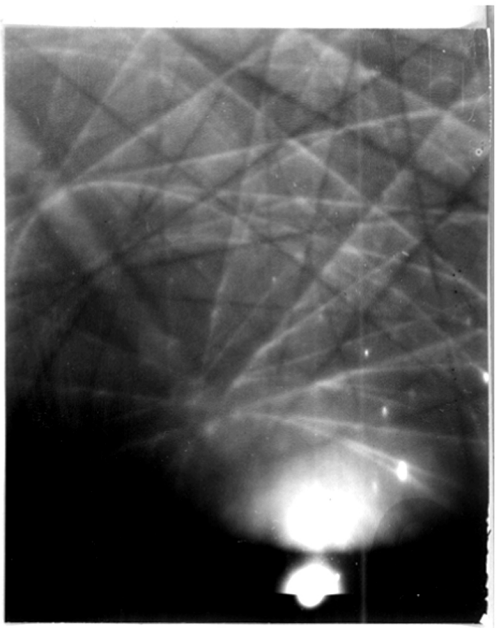

Figure 29. 30,000 A. deposit on Fe (310) face from sulphate bath at 80°C.

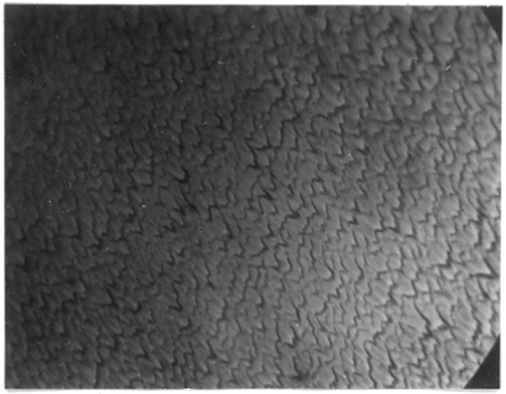

Figure 30. Micrograph of deposit of Figure 29.
x 940.

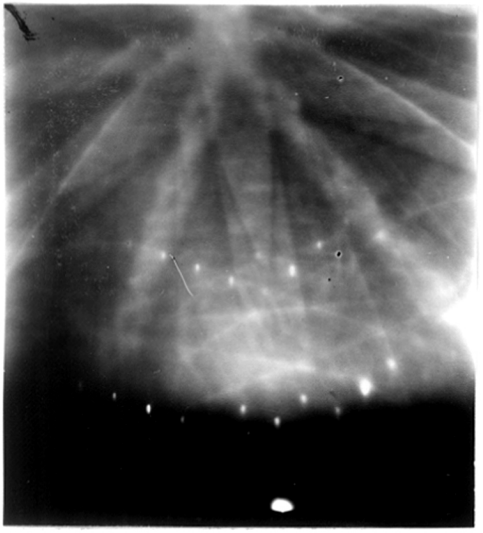

Figure 31. Electropolished Fe (321) face.

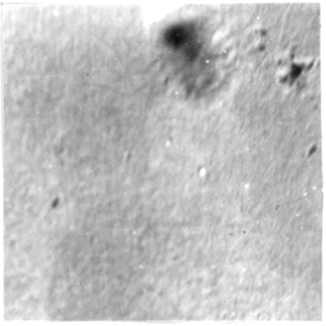

Figure 32. Electron micrograph of surface giving Figure 31.

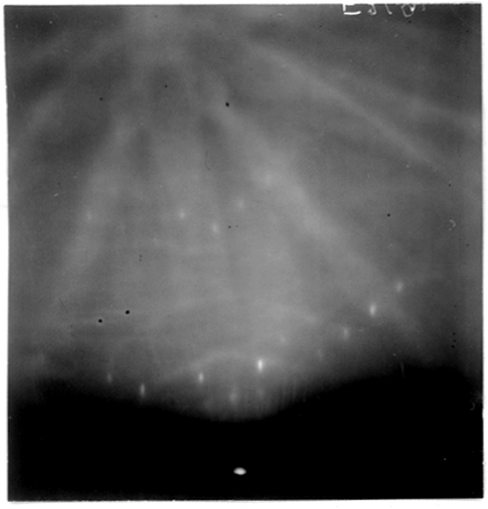

Figure 33. 5,000 A. deposit on Fe (321) face from sulphate bath at 80°C.

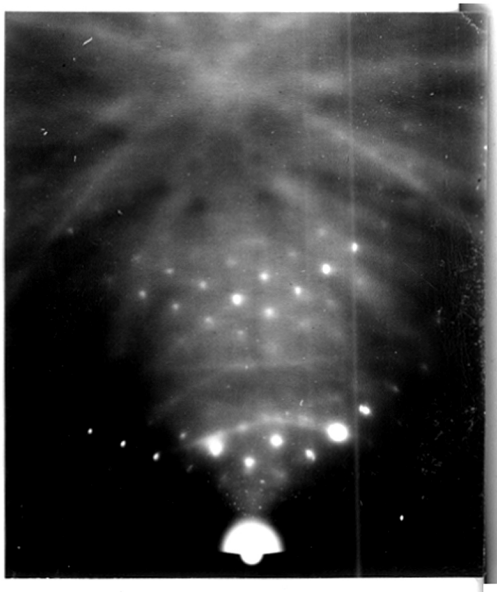

Figure 34. 30,000 A. deposit on Fe (321) face from sulphate bath at 80°C.

Figure 35. Micrograph of deposit of Figure 34.
x 455

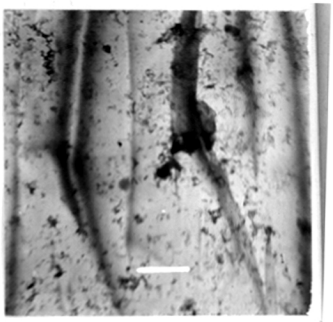

Figure 36. Electron-micrograph of deposi of Figure 34.

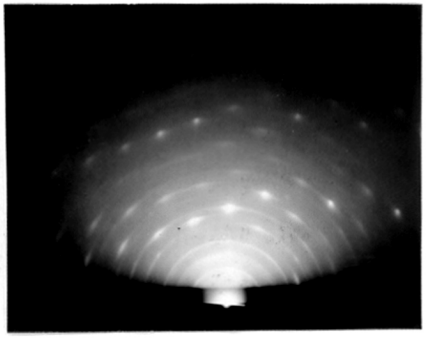

Figure 37. 500 A. deposit on Fe (321) face from sulphate bath at 20°C.

growths from the chloride bath. Deposition conditions favouring outward growth overcame, to a large extent, the substrate influence after a deposit thickness of only a few hundred angstroms had been reached (figure 37)

Iron deposited from the sulphate bath on to single crystals gave diffraction patterns with sharp Kikuchi lines and few spots showing that it had continued the structure of the substrate very faithfully and maintained a more or less atomically smooth surface. The surface tended to become more uneven as the deposit thickness increased, as is shown by the broadening of the Lane zones in figure 34 as compared with those in figure 33. There was no evidence of twinning in any of the patterns from these deposits. The micrographs of some of these deposits suggest that there is a tendency for preferential growth along [III] rows (which are the rows of highest atom frequency for iron). Thus, the direction of the spurs in figure 30, which is a micrograph of the deposit on a (310) face, are parallel to $[\bar{1}\bar{1}\bar{1}]$ which makes an angle of about 21° with the surface, and the ridges on the surface of the deposit on the (321) face (figure 35) are probably $\{110\}$ faces bounded by $\langle 111 \rangle$ edges. Figure 36 is an electron micrograph of part of the surface of the latter deposit.

The diffraction patterns from deposits on single crystals from the chloride bath, however, all show a large number of spots lying on broad Lane zones and are without

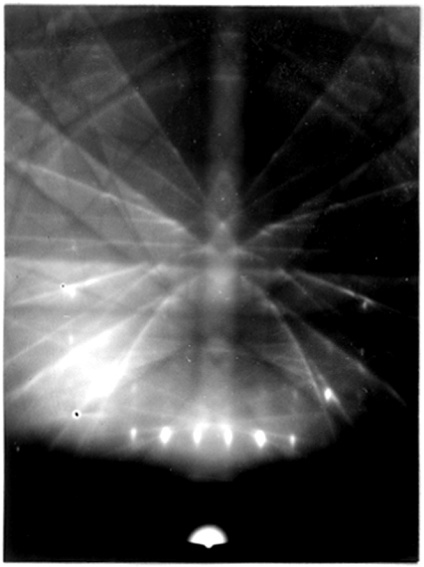

Figure 38. Electropolished Fe approx.(001) face. [110] in plane of incidence.

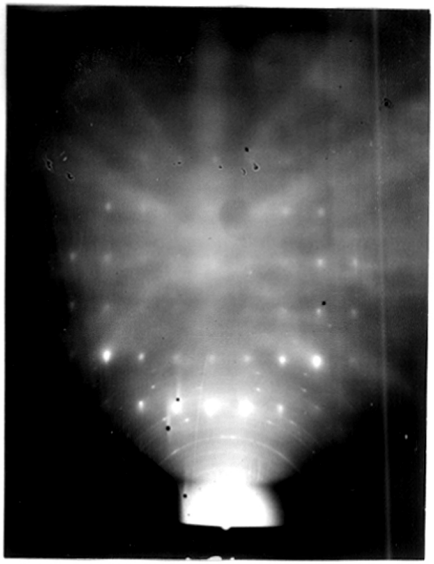

Figure 39. 50,000 A. deposit on Fe approx.(001) face from chloride bath at room temp.

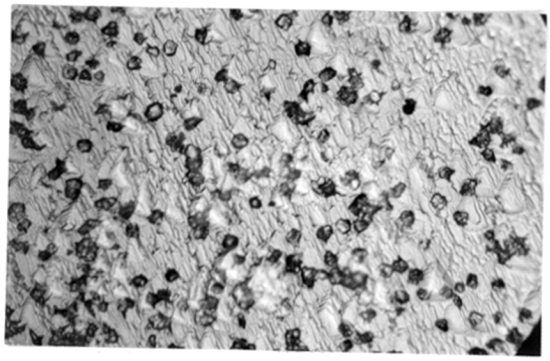

Figure 40. Micrograph of deposit of Figure 39.

X 455

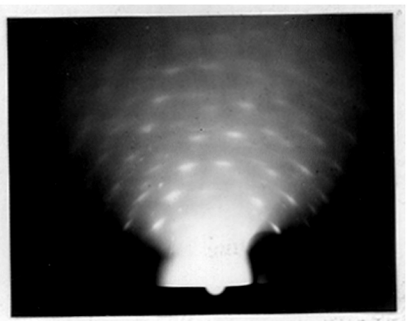

Figure 41. 50,000 A. deposit on Fe (321) face from chloride bath at room temp.

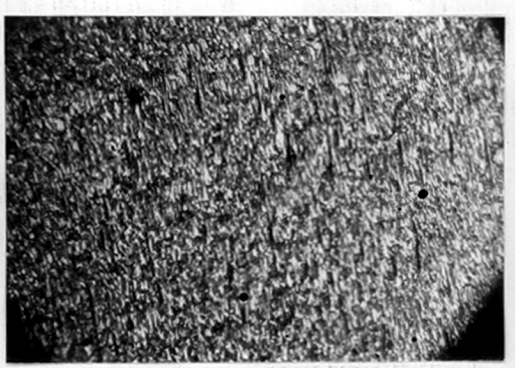

Figure 42. Micrograph of deposit of Figure 41.

x 455.

sharp Kikuchi lines, indicating that the surface was relatively rough. Most of the patterns also contain rings, mostly due to oxide, but some due to randomly disposed iron crystals. Extra spots probably due to twinning of some of the deposit crystals are also present in many of these patterns.

Figure 39, the pattern due to a deposit on a cube face, shows the $\sqrt{2}$-rectangle pattern associated with the cube face diagonal azimuth in its normal position, and also displaced by a rotation of 110° about the axis of the beam i.e. by 110° about [110]. This displaced component of the pattern corresponds to twinning of some of the deposit crystals following the substrate orientation on {111} or {112} planes. (These twins are identical as far as the lattices are concerned but Barrett [41] regards {111} twinning as being the correct description for face-centred cubic lattices and {112} as correct for body-centred cubic lattices.) The micrograph (figure 40) suggests that the deposit has grown in layers parallel to the substrate and bounded by cube edges.

The pattern, figure 41, from a 50,000 A thick deposit on a (321) face with the beam along $[\bar{1}11]$ shows a slight anticlockwise arcing of the spots and it is possible that stress set up during deposition was relieved by a process of "rotational slip" [42] on $(\bar{1}11)$ planes, though this pattern alone cannot be regarded as conclusive evidence of this. It was found later (Part III) that deformation of iron crystals corresponding to a rotation of lamellae parallel to

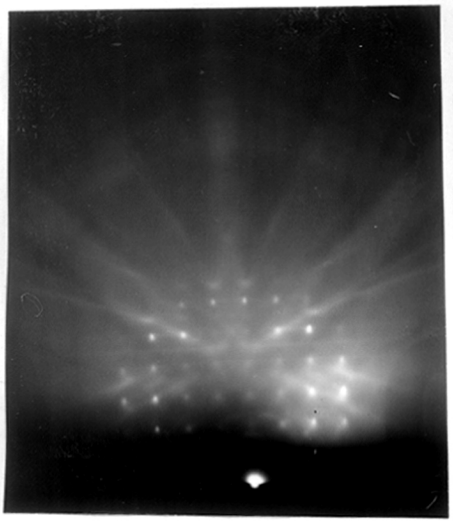

Figure 43. 200 A. deposit on Fe (110) face from chloride bath at room temperature Beam along [001].

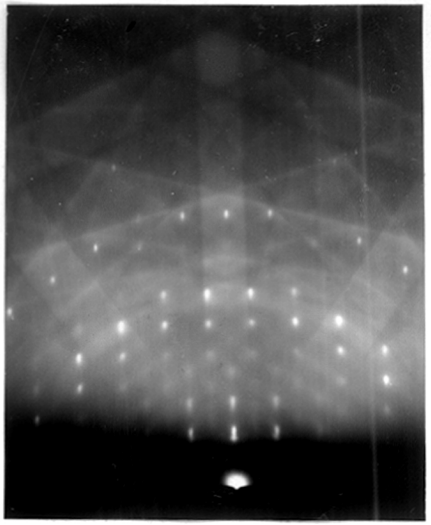

Figure 44. As Figure 43 but beam along [1$\bar{1}$0]

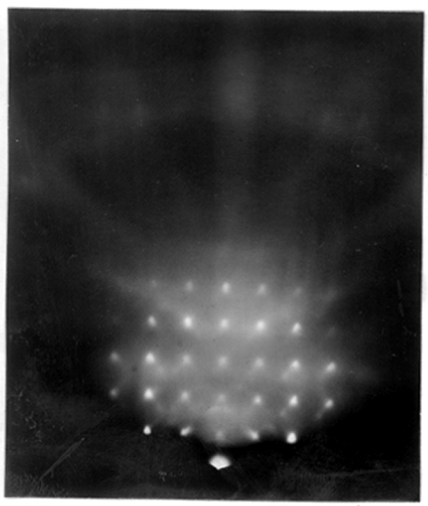

Figure 45. As Figure 43 but thickness of deposit 1000 A.

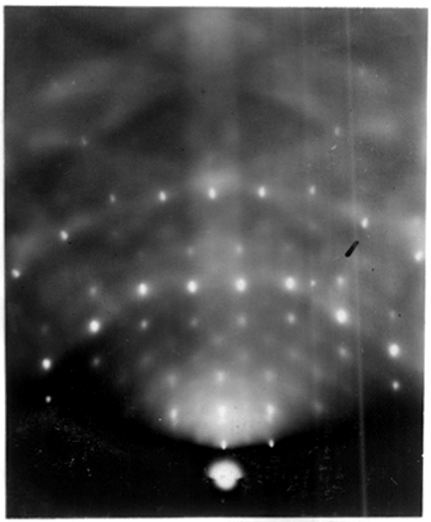

Figure 46, As Figure 45, but beam along [1$\bar{1}$0]

{111} planes about a ⟨111⟩ axis can occur. Figure 42 is a micrograph of this deposit.

The patterns from the deposits on the (110) face of iron are particularly interesting in that they show that the disturbances which appear to be inherent in deposition from the chloride bath occur even in the very earliest stages of growth. Figures 43 and 44 are the patterns from a deposit at room temperature of average thickness 200 A, and the relatively large number of spots shows that the surface had become uneven. The individual diffraction spots in the pattern at the cube-edge azimuth are slightly arrow-shaped, and some extra spots are just visible. These effects are shown much more clearly in figures 45 and 46 due to a deposit of 1,000 A average thickness. The angle at the tip of the arrow-shaped spots is about 53°, and the spot shape therefore corresponds to refraction of the diffracted beams at {310} facets developed on the deposit crystals.

A body-centred cubic space lattice gives a face-centred cubic reciprocal lattice of side $2a^*$, and figure 48 shows the projection of the reciprocal lattice of a [112] twin of iron on the cube face of the reciprocal lattice of the original crystal. If the beam is considered as directed along $-c^*$ (i.e. perpendicular to the plane of the diagram) then the distribution of points in the plane of the diagram (i.e. points for which $l = 0$) corresponds to the diffraction pattern appearing near the undeflected beam spot on the plate, and it will be seen that the points of the reciprocal lattice of

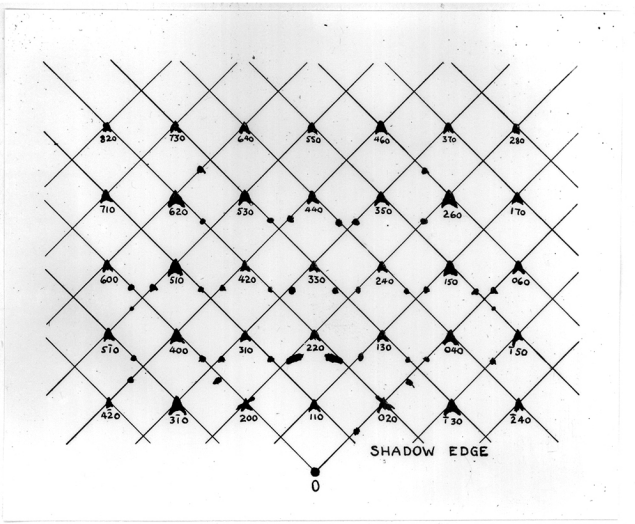

Figure 47. Diagram of Figure 45 showing indices of main diffractions.

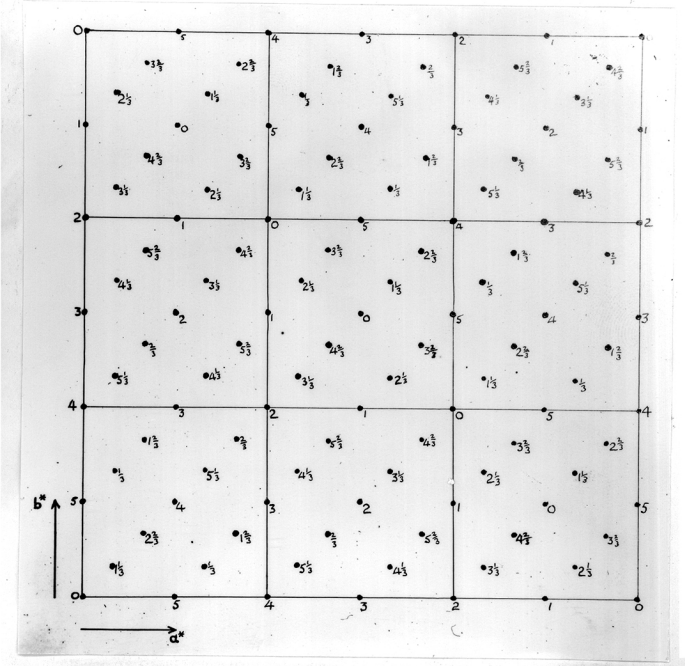

Figure 48. Projection of reciprocal lattice of [112] rotation twin on (001) plane of untwinned reciprocal lattice.

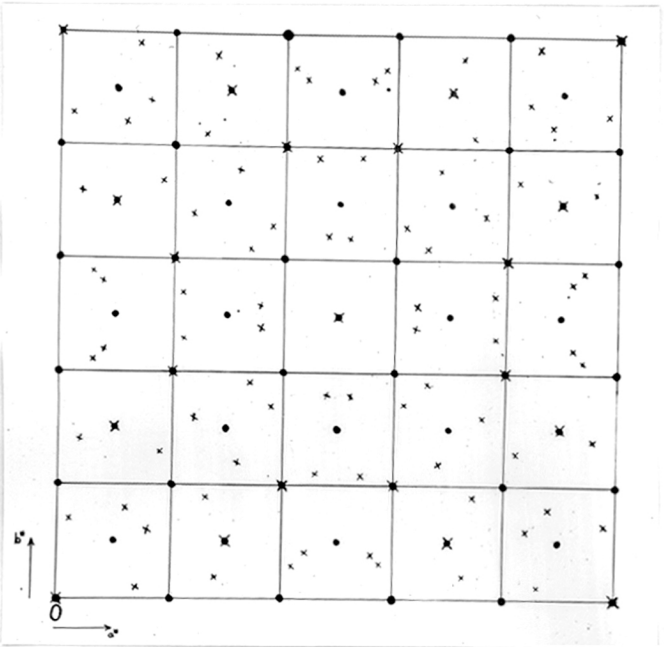

Figure 49. Reciprocal lattice points with $l = 0$ for untwinned lattice and for 310 rotation twins about axes in the plane of the diagram.

• = untwinned reciprocal lattice points

× = twinned reciprocal lattice points.

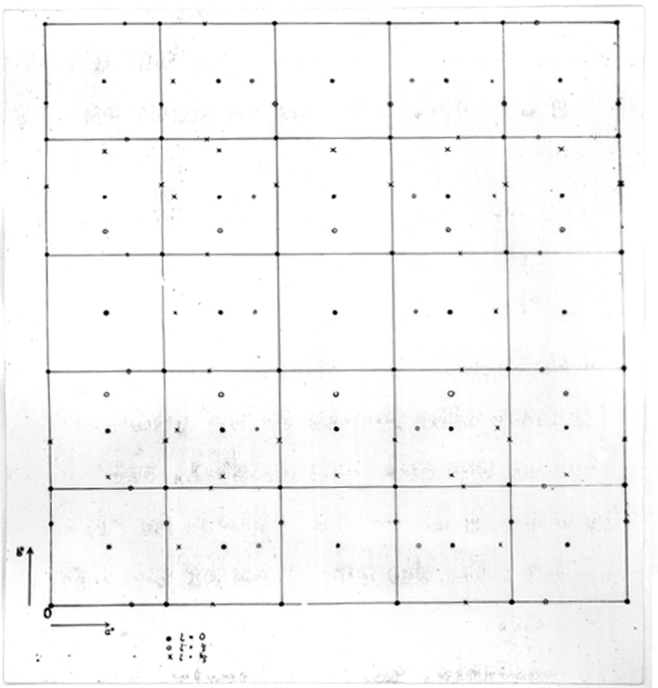

Figure 50. Reciprocal lattice points with l = 0, l = ± 1/5, and l = ± 2/5 of untwinned lattice and of lattices twinned by rotation about <310> axes not in plane of diagram projected on to (001) plane of untwinned reciprocal lattice.

the twinned crystal for which $\ell = 0$ are either at the corners or centres of the marked squares, and are therefore coincident with points due to the original lattice. It is also clear from a comparison of the reciprocal lattice diagram with figure 47 that the "extra" spots in figure 45 cannot be due to the occurrence of diffractions with low fractional indices of ℓ, e.g. $\ell = \pm \frac{1}{3}$ etc. Figure 49 shows some of the reciprocal lattice points with $\ell = 0$ for twins on $\{310\}$ planes parallel to the beam and perpendicular to the plane of the diagram, and it is clear that twins of this type cannot account for the "extra" spots. Twins on $\{310\}$ planes parallel to cube edges perpendicular to the beam give reciprocal lattices with points in the plane $\ell = 0$ coincident with points due to the original crystal, but the positions of the points with $\ell = \pm \frac{1}{3}$ and $\pm \frac{2}{3}$ shown in figure 50 are in partial agreement with the positions of the extra diffractions of figure 45.

It is possible, though unlikely, that the additional pattern is due to an epitaxial growth of an oxide on the iron deposit. However, a complete interpretation of the pattern of figure 45 has not yet been obtained.

Microscopical examination (figure 51) makes it clear that the roughness of the surface is the result of growth having proceeded from a small number of nuclei. A deposit at the same current density (~25 mA/cm^2) but at 70°C. yielded similar diffraction patterns, but figure 52 shows that the number of growing nuclei was about four times greater at this

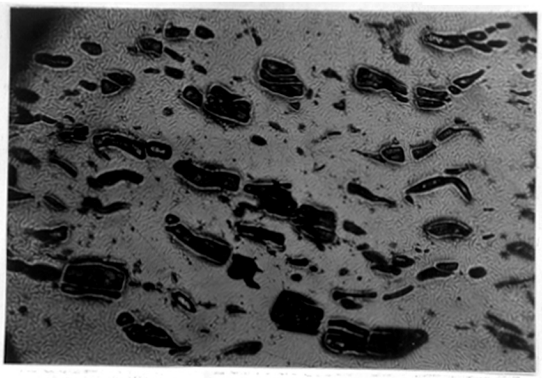

Figure 51. Micrograph of deposit of Figures 45 and 46. x 110

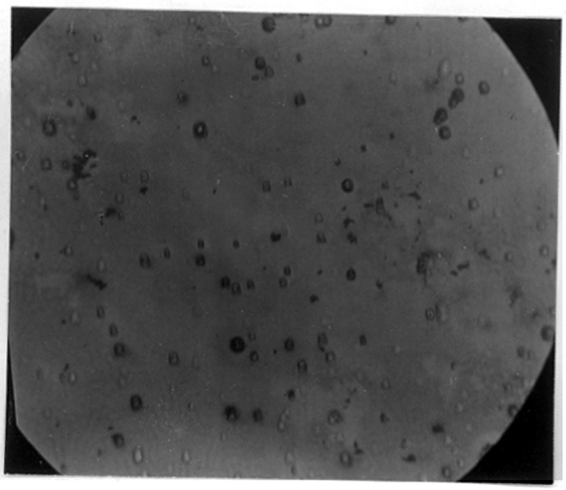

Figure 52. Micrograph of 750 A. deposit on Fe (110) face from chloride bath at 70°C. and 0.25 ma/sq.cm.

x 455.

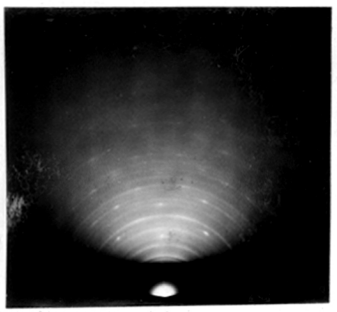

Figure 53. 55,000 A. deposit on Fe (110) face from chloride bath at room temperature. Beam along [110] at centre of specimen.

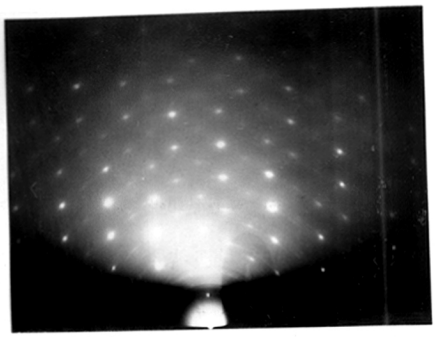

Figure 54. As Figure 53, but beam at edge of specimen.

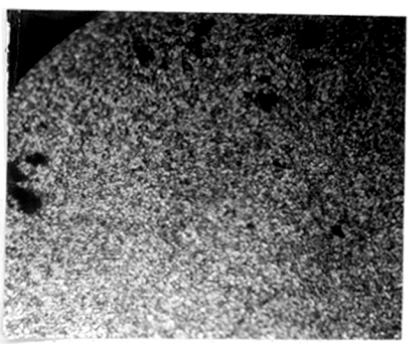

Figure 55. Micrograph of central region of deposit of Figures 53 and 54.
x 455.

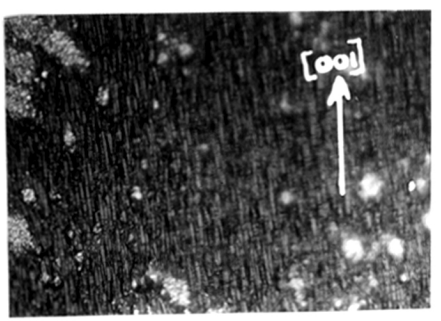

Figure 56. Micrograph of edge of same specimen.
x 455

higher temperature.

In a thick deposit (55,000 A) on a (110) face at room temperature, a number of the crystals had become disorientated, and a comparison of the diffraction patterns given by the centre and the edge of the specimen (figures 53 and 54 respectively) shows that this effect is more marked at the centre - a conclusion confirmed by microscopical examination (figures 55 and 56). Figure 56 shows that even near the edge of the specimen there are areas of random growth, and also that the epitaxial deposit crystals are elongated parallel to the cube edge. A deposit formed on the same face at 70°C. and 11 mA/cm^2 did not exhibit any difference between the growth at the edges and centre, and it therefore seems that the rate of supply of ions to the cathode region by diffusion (about three times greater at 70°C. than 20°C.) is of great importance, and it is to be expected that when the rate of diffusion is generally low the supply of ions will be less at the centre of a specimen than at the edges.

The diffraction pattern of this deposit formed at 70°C. also showed some extra spots as in other cases. The micrograph, figure 57, shows a double twin. The direction of the cube-edge in the larger twin makes an angle of about 110° with the cube edge of the original crystal (indicated by the arrow) and as the surfaces of the twinned and untwinned deposits are of the same height, and the direction in which

Figure 57. Micrograph of 22,000 A. deposit on Fe (110) face from chloride bath at 70°C. and 11 mA./sq.cm.
x 455

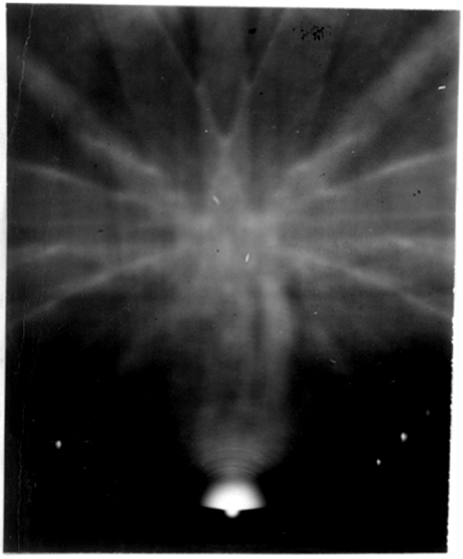

Figure 58. 12,000 A. deposit on Fe approx.(001) face from chloride bath at 70°C. and 6.7 mA/sq.cm.

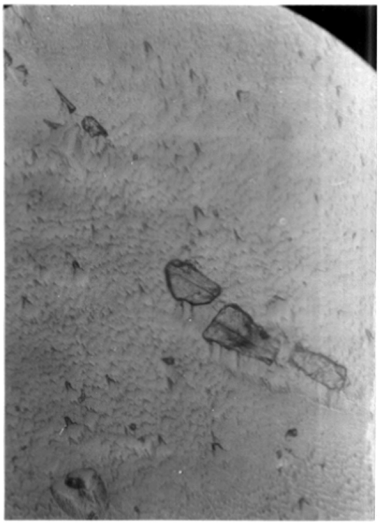

Figure 59. Micrograph of deposit of Figure 58.
x 455.

the specimen is viewed is parallel to [110], there is little doubt that the twin is of {112} type. The smaller triangular twin has a plane in common with and parallel to the cube-edge of the {112} twin and is probably a twin of the {112} twin.

Micrographs of deposits at room temperature on (001) and (110) faces (figures 40 and 56 respectively) and of the deposit at 70°C. on the (110) face (figure 57) all show the deposit crystals to be elongated parallel to the cube edge, and the direction of elongation of the spurs shown in figure 59, the micrograph of a deposit at 70°C. on a face about 10° of (001) is along [100], although there is a cube edge - namely [010] - actually in the surface. This apparent tendency for preferential growth parallel to the cube edge may be the result of growth along the densest atom rows, i.e. ⟨111⟩, being prevented by the prevailing bath conditions and therefore proceeding instead along the next most densely populated rows, i.e. ⟨100⟩. It could, however, also be the result of slight magnetization of the crystals, which would cause the deposit crystals to be aligned parallel to the cube edge.

Deposition of iron on polished mild steel. The evidence of Table IV for polycrystalline specimens may be summarized thus:

1. Lateral growth from the chloride bath occurs with low current densities at room temperature and relatively high current densities at higher temperatures.

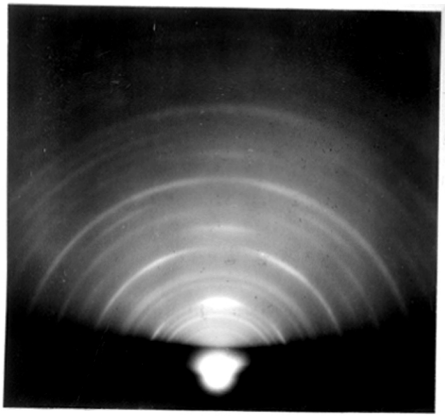

Figure 60. Fe deposited on polished mild steel from chloride bath at 50°C. and 11 mA/sq.cm. Thickness of deposit 21,000 A. (110) orientation.

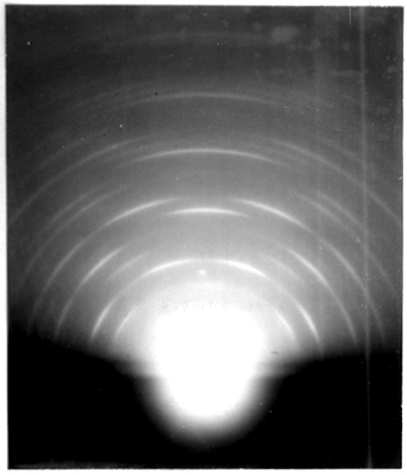

Figure 61. Fe deposited on polished mild steel from chloride bath at room temperature and 0.9 mA/sq.cm. Thickness of deposit 19,000 A. (111) orientation.

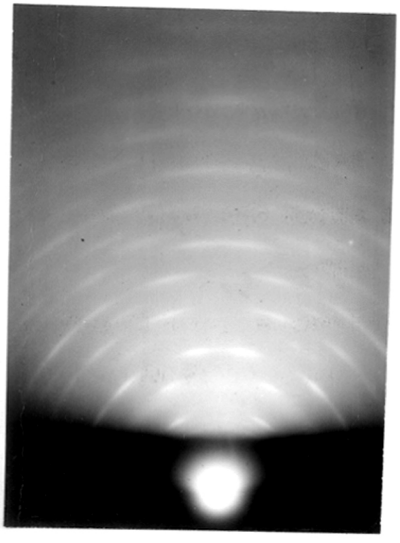

Figure 62. Fe deposited on polished mild steel from chloride bath at room temp. and 2 mA/sq.cm. Thickness of deposit 55,000A. (113) orien

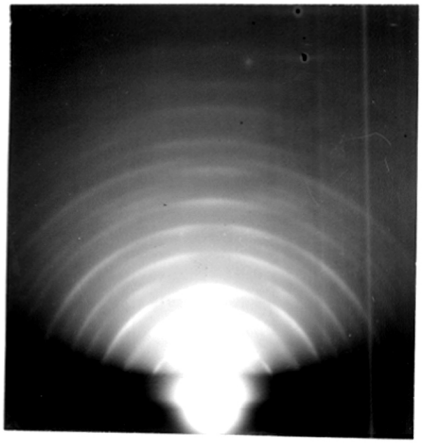

Figure 63. Fe deposited on polished mild steel at room temp and 20 mA/sq.cm. Thickness of deposit 46,000 A. (112) + (113) orientations.

2. Increasing the current density causes the current efficiency to fall and gives rise to deposits with various one-degree orientations other than that characteristic of simple outward growth, i.e. (111). Comparison of these patterns (figures 62 and 63) with the diagrams of figures 64 and 65 shows that the orientations are respectively (113) and a mixture of (112) and (113) orientations. These orientation axes are all of [11ℓ] type and the densest atom plane is therefore perpendicular to the surface in every case.
3. Increasing the area of the cathode does not affect the current efficiency, but mixed (112) and (113) orientations occur instead of (113) alone.
4. Dilution of the bath to half strength does not affect the current efficiency, but (111) orientation also occurs over the current density range giving (113) orientation in the concentrated bath, giving way to (112) and (113) orientations at about the same current density as in the concentrated bath.
5. Slight acidification with HCℓ causes a marked decrease in current efficiency and the occurrence of mixed (112) and (113) orientations throughout the range where other orientations are otherwise produced.

The occurrence of (112) and (113) orientations as different forms of outward growth cannot be regarded as the result of crystals growing along [111] atom rows into all possible regions of high cation concentration since the net effect of

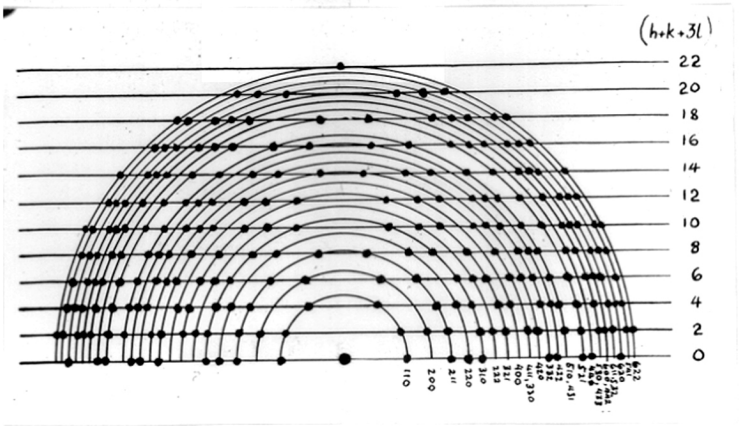

Figure 64. Theoretical positions of diffraction arcs due to body-centred cubic lattice in one-degree (113) orientation.

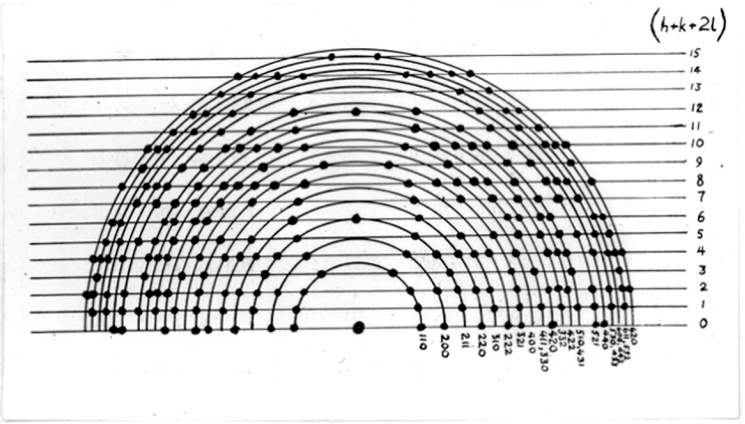

Figure 65. Theoretical positions of diffraction arcs due to body-centred cubic lattice in one-degree (112) orientation.

such growth would be the production of a random deposit.

The work with single crystal substrates suggests that twinning of crystals in (111) orientation might account for the appearance of (113) and (112) orientations. These last two orientations cannot be produced from (111), nor can (112) be produced from (113), by twinning on {112} planes, but crystals in (112) orientation could be produced from crystals in (113) orientation, and these in turn could be produced from crystals in (111) orientation, by twinning on {310} planes, in both cases with a disorientation of about $\pm 4^{\circ}$. There are several objections to this explanation. Firstly, not all the {310} twins of crystals in (111) orientation would be in (113) orientation with respect to the substrate, and it is difficult to account for the non-appearance of the orientations due to the other twins. Secondly, if twinning is the cause, crystals in (111) orientation should also appear together with the others, at least in the first layers of the deposit, but figures 69, 70 and 72, which are the patterns from deposits of 200 A, 1,000 A and 5,000 A thickness respectively formed under conditions for (113) orientation, show quite clearly that no such effect occurs. Far from the intensity of the 222 ring in the plane of incidence increasing in intensity to form an arc there, it decreases as the deposit becomes thicker. Thirdly, there seemed no reason why the process of twinning, once started, should not continue throughout the growth of the deposit which, initially random, would remain so. It is clear, therefore, that the bath conditions actually favour the growth

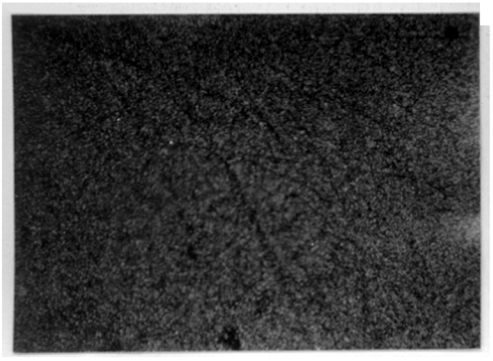

Figure 66. Micrograph of Fe (110) orientated deposit on on polished mild steel.
x 455

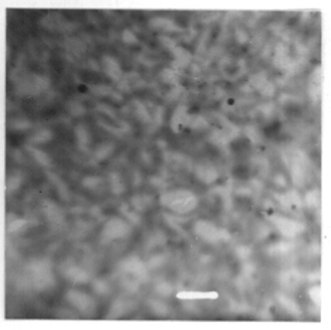

Figure 67. Electron micrograph of Fe (110) orientated deposit.

Figure 68. Micrograph of Fe (111) orientated deposit x 455

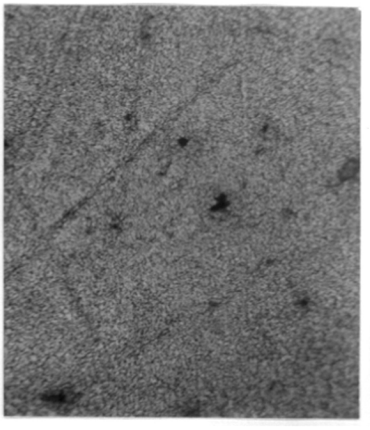

Figure 69. Micrograph of Fe (112) and (113) orientated deposits x 455.

of crystals in a particular orientation from the very beginning, especially since increase in deposit thickness causes an increase in sharpness of orientation.

The hydrogen co-deposited with the iron may have a considerable effect on the crystal growth not only by adsorption on the growing crystal faces, but by forming an interstitial solution, since it is known to dissolve much more readily in an iron cathode, and thus distort the iron lattice slightly. Strain set up in this manner might be relieved by twinning.

The work of Heyrovský [43] suggests that there may be a difference in the times taken for the ferrous ion to be discharged from the sulphate and chloride baths. Using an oscillographic method he found that the divalent ions of the transit elements exhibited cathodic polarization at a streaming mercury cathode, but reduction processes involving a transfer of only one electron occurred reversibly. He suggested that the transfer of more than one electron is not simultaneous but consecutive, e.g. $Fe^{++} + e \rightarrow Fe^{+}$ followed by a process he terms 'dismutation' $2Fe^{+} \rightarrow Fe + Fe^{++}$, and considered that the velocity of dismutation determined the rate of electro-deposition. He also deduced that this velocity was least for the transition elements, which fill up the valency electrons into lower electron shells, and was increased by heat and the presence of Cl^{-} ions but decreased by films of adsorbed molecules. The action of Cl^{-} ions was attributed to the fact that they are deformable in an electric

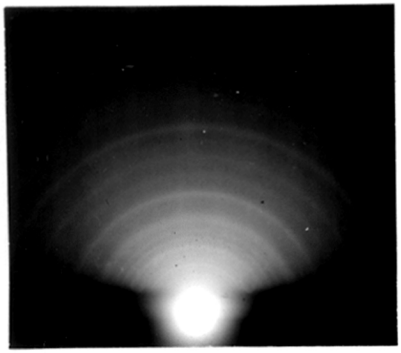

Figure 70. Fe deposited on polished mild steel from chloride bath at room temp. and ½ mA/sq.cm. Thickness 200 A.

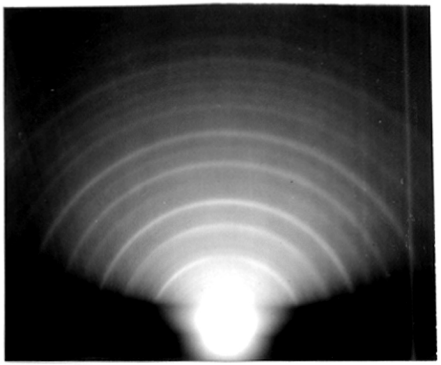

Figure 71. As Figure 70, but thickness of deposit 10000 A.

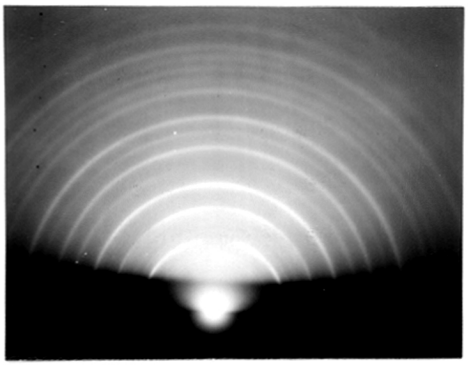

Figure 72. As Figures 70 and 71 but thickness of deposit 5,000 A.

field and a sort of electronic convection through the Cl^- ion occurred between the cathode and the cation being neutralized. SO_4^{--} ions have a rigid electronic structure and are not deformable. In order to act in this way it would be necessary for the Cl^- ions and cations to be in close association.

Miller [44] has considered the problem or ion-association in a bi-univalent electrolyte. Following his treatment it appears that in both baths (1) and (2) ion-triples and ion-pairs (of the form $FeCl^+$) are each about 100 times more numerous than free ions, but the ion-pairs are slightly more numerous than the triples. The total concentration of ions in bath (2) is of course only half that in bath (1).

It seems possible therefore that the rate of deposition of Fe^{++} ions relative to the rate of deposition of H^+ ions may be of importance in the growth of the electro-deposited crystals. The disturbance of the growth at high current densities will be increased by the fact that more hydrogen is deposited relative to iron from the chloride bath at increased current densities.

Hydrogen atoms will in general tend to be adsorbed in the positions of minimum potential energy on the growing crystals and thus hinder the iron atoms taking up those positions. If the time taken to discharge a Fe^{++} ion is comparatively great, the ions will be in close proximity to the cathode for a considerable period and be more likely to be discharged at positions of least potential energy. If

the discharge time is relatively small however, the atoms will have to be incorporated in the lattice in the most stable positions available at the moment of discharge and since the adsorption of hydrogen will prevent growth along [111], the crystals grow along less densely packed rows in the densest atom plane - namely, [113] and [112].

Dilution of the bath reduces the concentration of free and associated cations so that although the number of Fe^{++} ions relative to the number of H^{+} ions deposited per second is the same as in the concentrated bath, the discharge time will be greater since the degree of association is less, and (111) orientation continues until the rate of hydrogen discharge becomes great enough to cause growth along [112] and [113]. Acidification causes such a copious discharge of hydrogen that growth along [112] and [113] occurs even at quite small current densities. With a large cathode the diffusion to and from the centre is restricted and a higher concentration of Cl^{-} ions results, causing a greater association of the Fe^{++} and Cl^{-} ions. The discharge time is therefore reduced, and there is a tendency for growth along [112] as well as along [113]. Lateral growth occurs with relatively high current densities at higher temperatures because of the greater mobility of the ~~atoms~~ ions on the surface of the cathode and the decreased discharge of hydrogen.

PART THREE.

THE DEFORMATION OF IRON CRYSTALS BY UNIDIRECTIONAL ABRASION.

Part III. The Deformation of Iron Crystals by Unidirectional Abrasion.

Introduction.

It was recently established by Wilman [42] that a new deformation process, rotational slip, is common in crystals, and frequently occurs as the result of unidirectional abrasion of single crystal surfaces. Rotational slip has also been found in epitaxial growths. Thus, Evans and Wilman [45] found that it had occurred on $\{11\bar{2}0\}$ planes of ZnO formed by heating a zinc-blende (110) surface, Gharpurey [46] found that it occurred on cube faces of Ag grown epitaxially on the cleavage face of NaCl, and Goswami [47] found it on {110} planes of Cu_2O formed on the (110) face of a copper single crystal by immersion in NaOH solution at 75°C. and on $\{11\bar{2}0\}$ planes of Cd electrodeposited on a copper (110) face. In all these cases it seemed that the lamellae parallel to the specified planes, which were perpendicular to the surface, had rotated about an axis normal to them in order to relieve epitaxial stress due to differences in lattice spacings.

In view of the possibility that rotational slip had occurred in one of the electrodeposits of iron on an iron (321) face (see above, Part II) it was considered desirable to

investigate the possibility of deformation of iron crystals by rotational slip, and unidirectional abrasion seemed the most suitable method of trying to produce such effects.

Bénard and Lacombe [48] have examined by an X-ray reflection method iron crystals which had been subjected to abrasion, and obtained ring patterns which indicated that the surface of the crystal had become polycrystalline as a result of this treatment. Electropolishing of the surface to a depth of about 10 μ resulted in the rings of the X-ray pattern giving way to arcs characteristic of crystals in one-degree orientation. This in turn gave way to the original single crystal spot pattern after a total depth of about 60 μ had been removed by electropolishing. They also stated that the one-degree orientation produced was independent of the direction of abrasion, but in fact their results show the contrary.

Evans and Wilman have obtained results which were most easily interpreted as showing that rotational slip had occurred, as a result of unidirectional abrasion, in zinc blende on {110} planes and in copper on {001}, {110} and {111} planes [45].

Experimental.

The two crystal faces used in this work - (110) and (001) - were prepared as described in Part II by smoothing on emery paper and electrppolishing. Abrasion of these crystals on emery paper was carried out near the circumference of a disc about 20 cm. in diameter rotated at about 300 r.p.m. The crystals were held in recesses cut in brass cylinders and a light load (~ 150 gm.) was applied by hand.

After abrasion, or etching to a desired depth under electropolishing conditions, the crystals were etched for about 5 seconds in a 1% solution of picric acid in alcohol to remove any oxide layer, washed in a jet of acetone, and immediately immersed in n-propyl alcohol. They were then transferred, covered with alcohol, to the diffraction camera and this was at once evacuated.

Results.

For brevity the azimuths along and perpendicular to the abrasion direction are referred to as "A" and "B" respectively in the following account.

i. Abrasion of a (110) face along [1$\bar{1}$0] .

After abrasion for about 20 seconds on 0 emery paper and etching for a few seconds in picric acid, patterns such as

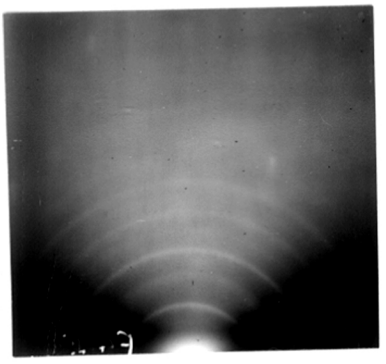

Figure 73. Fe (110) face abraded along [110] and etched for a few seconds in picric acid.

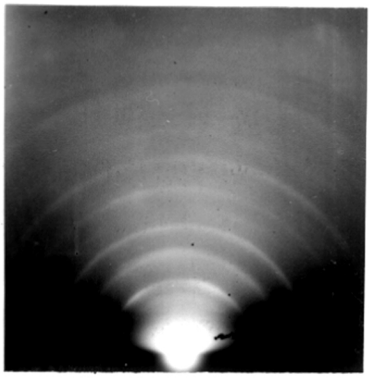

Figure 74. As Figure 73 but etched for 1½ minutes in picric acid. "B" azimuth.

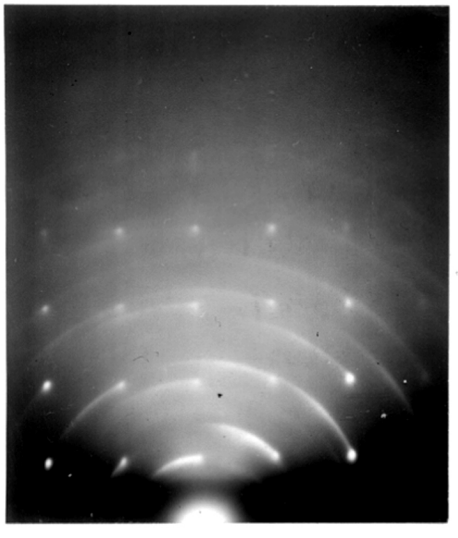

Figure 75. As Figure 74, but electropolished for 50 sec.

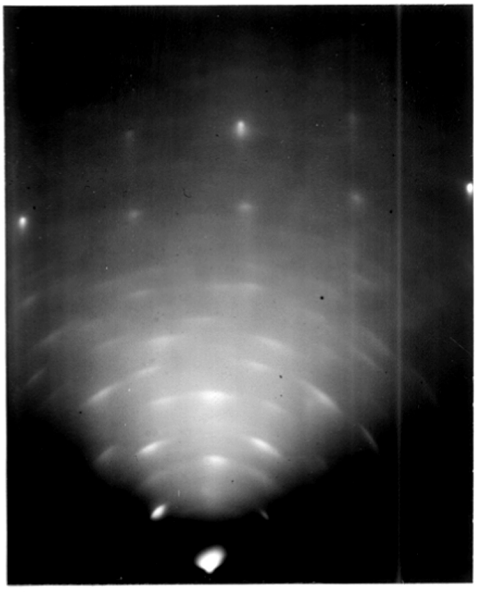

Figure 76. As Figure 75, but "A" azimuth.

Figure 73 were obtained at all azimuths, showing that the surface layers consisted almost entirely of a random polycrystalline iron. After further etching in picric acid for a total of 6½ minutes a diffraction pattern showing slight arcing of the rings was obtained at the "B" azimuth (Figure 74). The crystal was then partially electropolished for 50 seconds and the patterns of Figures 75 ("B" azimuth) and 76 ("A" azimuth) were obtained.

Figure 75 shows clearly the square spot pattern associated with this azimuth (the cube edge) of the undistorted crystal, together with circular arcs drawn out from the spots, indicating rotations of parts of the lattice by as much as 40° from the initial orientation. The absence of diffractions other than these strong hk0 spots and arcs shows that parts of the lattice in the surface regions were rotated about an axis which was parallel to the beam or nearly so, i.e. in the "B" azimuth direction. Figure 76 is in agreement with this conclusion since it contains, in addition to the spots and Kikuchi lines due to the undistorted crystal, rows of arcs which lie on layer lines parallel to the main nearly vertical spot rows. The arcs which appear correspond to a rotation of the same order of magnitude as that deduced from Figure 75, and their length shows a range of disorientation of $\pm$ 6° from the undistorted crystal, about an axis parallel to the "A" azimuth.

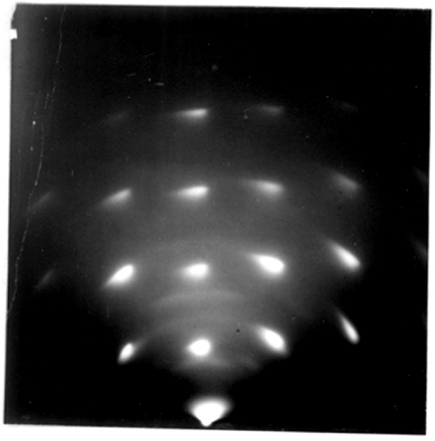

Figure 77. As Figure 75, but electropolished for further 20 seconds.

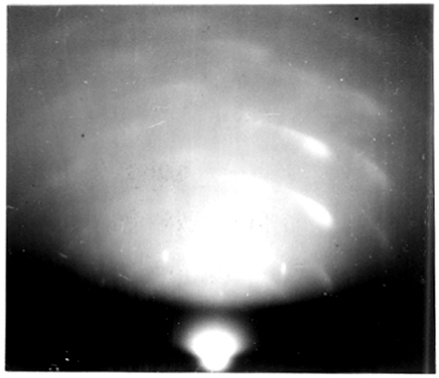

Figure 78. Fe {110} face abraded along [112] and electropolished for 75 seconds. "B" azimuth.

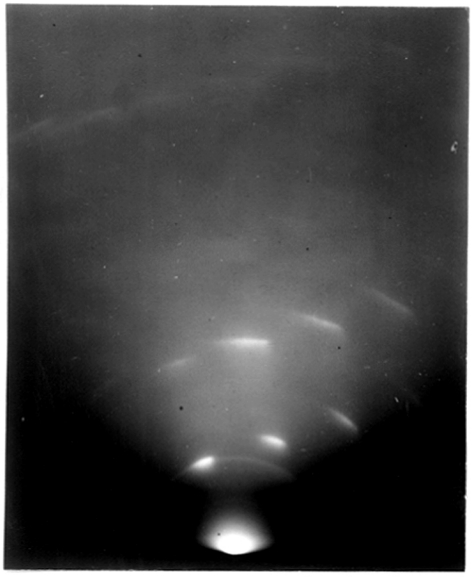

Figure 79. Fe (001) face abraded along [110] and electropolished for 2 minutes. "B" azimuth.

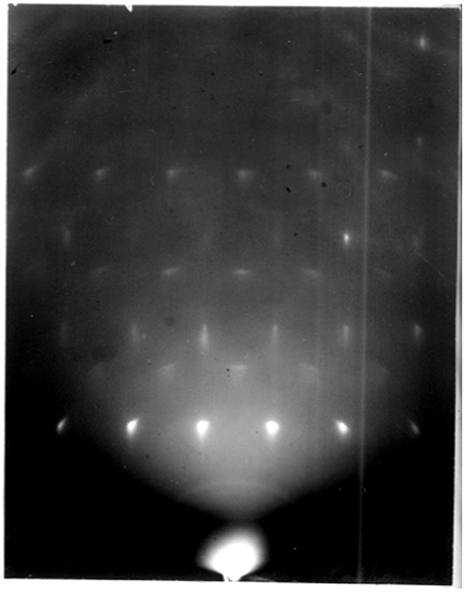

Figure 80. As Figure 79 but "A" azimuth.

The crystal was electropolished for a further 20 seconds and Figure 77 was obtained at the "B" azimuth. This is similar to Figure 75, but with shorter arcs tailing off from the spots, and there is more prominent drawing out of the spots and arcs near the shadow edge and normal to it, because of refraction at the surface which was then atomically smooth over small areas.

ii. Abrasion of a (110) face along $[1\bar{1}2]$.

After abrasion on 0 emery paper along $[1\bar{1}2]$ followed by electropolishing for 75 seconds, Figure 78 was obtained at the "B" azimuth. The sharp, slightly elongated spots near the shadow edge correspond to the undistorted crystal and form a regular hexagonal pattern. The more extensive pattern of strong "tailed" arcs which subtend about 20° at the undeflected beam spot, corresponds to such a hexagonal pattern rotated about the beam, i.e. about the "B" azimuth direction. The head of each arc begins after a displacement of about 5° from the corresponding spot of the undistorted crystal pattern, thus it appears that in the region grazed by the beam the crystal surface region had been rotated by this amount before being split up further into a range of rotated parts which gave the arc pattern. Since there are no other strong diffractions in the pattern the rotation axis is clearly closely along the "B" azimuth direction.

iii. Abrasion of an approximately (001) face along [110].

Abrasion on grade 0 emery yielded inconclusive results, so the face was abraded further with a coarser grade (F) and smoothed on grade 0 emery paper. It was then electropolished for 2 minutes and Figure 79 was obtained at the "B" azimuth. This figure shows only arcs corresponding to the normal $\sqrt{2}$-rectangle spot pattern rotated through 15° about the beam direction. The arcs on the narrow first-order circular Laue zone (about 7.3 cm. radius and centred near the undeflected-beam spot) define the axis about which rotation of parts of the crystal had occurred as being closely normal to the $(1\bar{1}0)$ planes.

Figure 80 was obtained at the "A" azimuth and showed faintly Kikuchi bands from the undistorted crystal, including the vertical one due to the $(1\bar{1}0)$ planes. The vertically-elongated (refracted) spots near the middle of the figure form a $\sqrt{2}$-rectangle pattern lying on the circular Laue zone centred near the middle of the top of the figure, where the [110] lattice row intersected the plate, and they are also due to the undistorted crystal. The rotation indicated by Figure 79 has evidently caused this pattern to be extended over a larger region and has caused the appearance of other short arcs lying on vertical rows between the spot rows of the original pattern. (The rings appearing near the shadow edge were due to a slight oxidation of the surface).

Discussion.

The experiments described above show that abrasion of electropolished iron crystals parallel or nearly so to planes of type {001}, {110} or {111}, which are normal to the surface or steeply inclined to it, causes rotations up to 30 or 40° of parts of the crystal about a clearly defined axis which lies normal to the {001}, {110} or {111} planes respectively.

These rotations of parts of the iron lattice near the surface appear to be inexplicable in terms of the hitherto-known directions of translational slip along <111>, usually on {110} at room temperature but sometimes on {112} or {123}, or of flexure. As in the case of copper [45] the results are most simply interpreted by a coherent fragmentation by rotational slip [42] occurring on the planes normal to the rotation axis; but with increasing rotation the flexure of the rotational-slip lamellae also increases as shown by the arcing in the "A" azimuth patterns. Again as in the case of copper, this view is well supported by direct microscopic and X-ray evidence [41,49,50] of the existence of lamellar "deformation bands" parallel to {100} or {111} planes in elongated or compressed iron. The orientation of the lattice in these bands at low deformation corresponded only to rotational slip of these lamellae over each other on their contact planes [42]. At

higher deformations microscopic examination showed that the lamellae became curved by flexure, and the orientations of the lattice in neighbouring lamellae were related in a more complex manner, apparently because of different combinations of translational slip in the adjacent lamellae.

Thus it seems that the abrasive particles exert in front of them a high compressive stress on the crystal (cf. Figure 5, reference [51]) and cause first a coherent lamellar fragmentation by the rotational slip process outlined above, and then, with the increasing pressure, a further disorientation probably by translational types of slip in the lamellae, which reduces still further the cohesion between neighbouring lamellae across their contact faces. This then facilitates removal of material as the abrasive particles continue their advance. This process amounts to the development of "deformation bands" such as those described by Barrett.

Channel-shaped scratches are left behind, at the sides of which, especially, there must also remain a fine-lamellar rotational slip zone. This slip must have been increased by the more or less tangential drag of the abrasive particles on the atomic planes to which these side faces approximate (cf. the macroscopic demonstration of rotational slip in $K_4Fe(CN)_6 . 3H_2O$ by frictional forces [42].

Finally, it is significant that the rotation caused by the abrasion was found to be particularly easy and extensive on {100} planes of iron, which are the reported fracture planes, and the close relationship of rotational slip to cleavage [42] is thus well exemplified in the present case.

GENERAL DISCUSSION.

General Discussion.

Electrodeposition can be used to study crystal growth under completely controlled conditions. The rate of growth can be continuously varied by varying the current density, and growth can even be stopped completely for a time and then continued later. Furthermore, the Brownian movement of the electrolytic solution gives the ions a mobility over the cathode surface far greater than deposited atoms would possess on the substrate at the same temperature. In spite of these facts, comparatively little systematic fundamental research has been carried out on the growth of electrodeposits.

Blum and Rawdon [52] considered the general problem in 1923, and their paper was probably the best published survey available at that time. They were, however, handicapped by the lack of the detailed and conclusive information about crystal habit and structure which could only be yielded by electron diffraction and which has since been obtained by Finch and his collaborators. This information combined with a precise knowledge of the deposition conditions has enabled a clearer picture of the fundamental mechanisms of electrodeposition to be formed. In the present work, the actual growth of electrodeposited silver crystals has been observed by microscopy, and the structure of deposits on iron single crystals and the effect of varying the bath conditions on the orientation of polycrystalline deposits on mild steel

have been investigated by means of electron diffraction.

It was found in the case of silver that at moderately high current densities, when ionic concentration becomes the chief controlling factor, the crystals grew most rapidly in directions parallel to <110>, i.e. along the directions of highest atom frequency. At lower current densities the crystals showed a more uniform development, and at higher current densities the crystal size was very much reduced and the deposit formed a loose conglomerate. What appears to be a general rule for most types of crystal growth, namely that the rates of growth in different directions are more nearly equal the greater the overall rate of crystallization [53], is evidently not true for electrolytically-grown crystals when ionic concentration is the controlling factor. This needle and fern like growth of silver is clearly very similar to the lead "trees" grown by Evans [54] under conditions of low ion concentration by resting the edge of a vertical sheet of zinc on a filter paper soaked in a 10% solution of lead acetate. After some time it was found that lead was only being deposited on the tips of the dendrites at distances of as much as 1 cm. from the zinc, and the use of ammonium sulphide as an indicator showed that the concentration of lead ions near the zinc sheet was almost zero.

The results for the electrodeposition of iron agree with the general conclusion that crystals grow by the addition of fresh material at the edges of layers parallel to the most

densely packed plane, since in all cases the crystals appear to grow parallel to atom rows in this plane. Under conditions of fairly rapid hydrogen evolution, however, growth along directions of highest atom frequency appears to be prevented, and growth occurs instead along other less densely populated rows.

When the rate of deposition of iron is not too great, and the ions have sufficient mobility over the surface, polycrystalline deposits grow so that they have the most densely packed atomic plane parallel to the substrate, and deposits on single crystals of iron continue the structure of the substrate to considerable thicknesses. The co-deposition of hydrogen, however, interferes with the process of growth, and is probably the cause of twinning and disorientation in the deposit. This twinning occurs even in the initial stages when the deposit still consists of separate nuclei. The number of these nuclei from which growth proceeds increases at higher temperatures.

The polycrystalline deposits under various bath conditions show that the nature of the anion is of great importance. It has long been known that the formation of complex ions, e.g. $Ag(CN)_2^-$, has a profound effect on the growth and form of electrodeposited metals, and it seems that in the deposition of iron from chloride baths ion association plays an important role, possibly by affecting the time of neutralization of the ferrous ions. The iron

group of metals all show high deposition overvoltages at room temperatures [55] and low hydrogen overvoltages. A general consideration of the relation between deposition overvoltage, hydrogen overvoltage and work function of a number of metals appears to support the slow neutralization theory [56]. Further research is necessary before this problem can be completely resolved, however.

The mechanism of crystal growth by electrodeposition has been treated theoretically by Gorbunova and Dankov [20] in terms of the time and work necessary for the formation of new two-dimensional nuclei, and the lateral extension of existing ones on a single crystal face. According to their analysis the overvoltage at each face should show a periodic variation, but because of concentration polarization and the large number of crystals involved the average overvoltage of a cathode actually maintains a steady value under constant conditions.

The importance of the study of the electrodeposition of metals because of its commercial applications has long been realized, but has resulted in much of the research carried out being of an empirical nature. It is to be hoped that the increasing knowledge of the operation of the various factors in the electrolytic bath and influence of the substrate will result in an increase in the more fundamental research into the mechanism of electrodeposition leading to further knowledge of crystal growth.

Acknowledgements.

The author thanks Professor G.I.Finch, M.B.E., F.R.S. for his much valued help and encouragement throughout the course of this work, and Dr.H.Wilman for many helpful discussions.

The author also thanks the Ministry of Education for an award under the Further Educational Training Scheme which enabled him to devote his whole time to this research.

References.

1. Thomson, Proc.Roy.Soc., 1931, A.133, 1.
2. Glocker and Kaupp, Z.Physik, 1924, 24, 121.
3. Bozorth, Phys.Rev., 1925, 26, 390.
4. Wood, Proc.Phys.Soc., 1931, 43, 138.
5. Frohlich, Clark and Aborn, Trans.Am.Electrochem.Soc., 1926, 49, 369.
6. Finch and Sun, Trans.Faraday Soc., 1936, 32, 852.
7. Finch and Williams, Trans.Faraday Soc., 1937, 33, 564.
8. Finch, Wilman and Yang, Disc.Faraday Soc., 43A, 144.
9. Yang, Ph.D.Thesis, University of London.
10. Cochrane, Proc.Phys.Soc., 1936, 48, 723.
11. Clark, Pish and Weeg, J.Appl.Phys., 1944, 15, 193.
12. Gardam, Disc.Faraday Soc., 43A, 182.
13. Finch and Wilman, Ergeb.exakt.Naturwiss., 1937, 16, 353.
14. Frary, Trans.Am.Electrochem.Soc., 1913, 23, 25.
15. Le Blanc, Abl.d.Deutsche Bunsen Ges., 3, 1910.
16. Aten and Boarlage, Rec.Trav.Chim.Pays-Bas, 1930, 39, 720.
17. Wernick, Trans.Faraday Soc., 1928, 24, 361.
18. Hoekstra, Rec.Trav.Chim.Pays-Bas, 1931, 50, 339.
19. Vahramian, Acta Physiochim.URSS., 1944, 19, 148.
20. Gorbunova and Dankov, C.R.Acad.Sci.URSS, 1945, 48, 15.
21. Fischer, Z.Metallkunde, 1948, 39, 161.
22. Montoro, Per.Min., 1938, 9, 55.
23. Coffin and Tingley, J.Chem.Phys., 1949, 17, 502.

24. Gorbunova and Vahramian, C.R.Acad.Sci.URSS, 1934, 2, 128.

25. Haring and Blum, Trans.Am.Electrochem.Soc., 1923, 44, 513.

26. Glasstone, Introduction to Electrochemistry, New York; D.van Nostrand 1942.

27. Watts, The Electrician, Nov. 11 and 25, Dec. 16 and 30, 1887; Jan. 13, 1888

28. Hughes, Trans.Am.Electrochem.Soc., 1921, 40, 185.

29. Burgess and Watts, Trans.Am.Electrochem.Soc., 1906, 9, 229

30. Muller, Metallurgie, 1909, 6, 145.

31. Stead and Carpenter, J.Iron Steel Inst., Sept., 1913.

32. Storey, Trans.Am.Electrochem.Soc., 1914, 25, 529.

33. Hughes, Trans.Faraday Soc., 1922, 17, 442.

34. Ruder, Trans.Am.Electrochem.Soc., 1921, 39, 451.

35. Kaspar, J.Res.Nat.Bur.Stand., 1937, 18, 535.

36. Thomas, Trans.Electrochem.Soc., 1943, 84, 305.

37. Städdard, Trans.Electrochem.Soc., 1941, 80, 499.

38. Larson, Moulton and Putnam, J.Electrochem.Soc., 1949, 95,86C

39. Kreiger, Bull.Soc.Franc.Elect., 1942, 2, 221.

40. Jacquet and Roquet, C.R.Acad.Sci.Paris, 1939, 202, 1012.

41. Barrett, The Structure of Metals, New York:McGraw Hill, 1943.

42. Wilman, Nature, 1950, 165, 321.

43. Heyrovský, Disc.Faraday Soc., 1947, 43A, 292.

44. Miller, Trans.Faraday Soc., 1939, 35, 691.

45. Evans and Wilman, Proc.Phys.Soc., 1950, A63, 298.

46. Gharpurey, Ph.D.Thesis, 1950, University of London.

47. Goswami, Ph.D.Thesis, 1950, University of London.

48. Bénard and Lacombe, Métaux et Corrosion, 1946, 21, 30.

49. Barrett, Amer. Inst. Min. Metall. Engrs., 1938, Tech. Publ. No. 977 (and Trans. A.I.M.E. 135, 296).

50. Barrett and Levenson, Amer. Inst. Min. Metall. Engrs., Tech. Publ. No. 1038 (and Trans. A.I.M.E., 135, 237).

51. Finch, Proc. Phys. Soc., 1950, B63, 465.

52. Blum and Rawdon, Trans. Am. Electrochem. Soc., 1923, 44, 397

53. Egli and Zerfoss, Disc. Faraday Soc., 1949, 5, 61.

54. Evans, Chem. and Ind., 1925, 44, 812.

55. Glasstone, J. Chem. Soc., 1926, 1887.

56. Bockris, Nature, 1947, 159, 539.